A bijection for nonorientable general maps

Jérémie Bettinelli

A bijection for nonorientable general maps

Jérémie BETTINELLI[†]

February 17, 2016

Abstract

We give a different presentation of a recent bijection due to Chapuy and Dołęga for nonorientable bipartite quadrangulations and we extend it to the case of nonorientable general maps. This can be seen as a Bouttier–Di Francesco–Guitter-like generalization of the Cori–Vauquelin–Schaeffer bijection in the context of general nonorientable surfaces. In the particular case of triangulations, the encoding objects take a particularly simple form and this allows us to recover a famous asymptotic enumeration formula found by Gao.

Keywords: map, graph, bijection, nonorientable surface, triangulation, Brownian surface.

1 Introduction

1.1 Motivation

The study of maps has seen tremendous developments in the past few decades. One of the reasons is that they provide natural discrete versions of a given surface. In particular, when taken according to a well-chosen natural probability distribution, it has been shown for several models that a random map converges (after scaling, in a certain sense) toward a limiting object. This limiting object is a random metric space and has (almost surely) the same topology as the surface on which the considered maps are drawn. It is called the *Brownian map* when the surface is the sphere, and the *Brownian* $\mathcal{S}$ for a general orientable surface $\mathcal{S}$.

In the most-studied case of the sphere, it has been shown [LG13, Mie13] for example that a uniform quadrangulation (map with only faces of degree 4) with n faces converges to the Brownian map as $n \to \infty$. See also [BLG13, ABA13, BJM14, Abr13] for other natural models of maps drawn on the sphere that exhibit the same behavior. An important aspect of these results is that the limiting object is universal, in the sense that it is always the Brownian map (up to a scale constant), independently of the model one considers. The case of a more general compact orientable surface (with a boundary allowed) has been studied, mostly in the context of uniform quadrangulations: partial convergence has been established in a series of papers ending with [Bet14] and a full convergence is under investigation [BM16]. The full convergence in the particular case of the disk has recently been shown in [BM15], where many more models are also considered.

[†]CNRS & Laboratoire d'Informatique de l'École polytechnique; jeremie.bettinelli@normalesup.org; www.normalesup.org/~bettinel.

All the previously mentioned results strongly rely on powerful bijective encodings of the considered maps. It turns out that quadrangulations are particularly well behaved with respect to these bijective encodings and this is the main reason why they are usually the first to be studied. However, if one wishes to study other models and, in particular, surfaces with a boundary, one needs more general bijective encodings. In the case of compact orientable surfaces, the so-called *Schaeffer-like bijections* [CV81, Sch98, BDG04, CMS09, AB13] allow one to conduct most studies. Note that, in certain cases, bijections of a different kind [PS06] have also been used [ABA13].

Until very recently, no such bijections were known in the case of a nonorientable surface. In [CD15], Chapuy and Dołęga took the first step by exhibiting a bijection allowing to encode nonorientable bipartite quadrangulations. In this work, we give an alternate description of their bijection, which provides an explicit construction for pointed quadrangulations[1] and we show how to generalize it to nonorientable general maps. These works lay the bases for the future study of nonorientable Brownian surfaces [BCD16].

Another cause of interest for maps is their remarkable enumerative properties. In fact, although maps are intricate objects by nature, many classes of them possess a quite simple enumerative structure. Thanks to different involved enumeration techniques (generating functions, matrix integrals, algebraic combinatorics), many classes of maps have been enumerated and map enumeration has become over the years a full-fledged research domain.

In the case of the sphere, Tutte [Tut63] gave a very simple closed formula for the number of rooted maps with a given number of edges. A bijective proof of this formula was given by Cori and Vauquelin [CV81] and later popularized by Schaeffer [Sch98]. It relies on their so-called *Cori–Vauquelin–Schaeffer bijection* encoding quadrangulations of the sphere with trees whose vertices carry integer labels satisfying local constraints. For more general surfaces, Bender and Canfield [BC86] showed that the number of rooted maps with n edges on a given surface (orientable or not) is asymptotically equal to a constant times $n^{5(h-1)/2}12^n$, where h is the type of the considered surface and the constant depends on the surface. Extending the Cori–Vauquelin–Schaeffer bijection, a combinatorial interpretation of this fact in the orientable case was given by Chapuy, Marcus and Schaeffer [CMS09]. Their approach rely on a bijection between bipartite quadrangulations (it is a classical simple fact that bipartite quadrangulations are in bijection with general maps) and one-face maps of the same surface, whose vertices carry integer labels satisfying some local constraints.

In parallel, Bouttier, Di Francesco and Guitter [BDG04] extended the original Cori–Vauquelin–Schaeffer bijection to encode maps of the sphere with an arbitrary face degree distribution. Unifying both aforementioned extensions, Chapuy [Cha09] proved similar asymptotic enumeration results for more families of maps on an orientable surface.

Nonorientability does not causes too much difficulties for generating function approaches. In addition to Bender and Canfield's results, we may cite the work of Gao, who showed [Gao91] that the number of rooted triangulations with n edges on a given surface (orientable or not) is asymptotically equal to a constant (depending on the surface) times $n^{5(h-1)/2}(12\sqrt{3})^n$. He also studied the algebraicity of the generating function of rooted maps on a given surface with face degree constraints [Gao93].

In their recent work [CD15], Chapuy and Dołęga extended the construction of [CMS09] to bipartite nonorientable quadrangulations. In this paper, we give a different construction of their

[1] A *pointed map* is a map given with a distinguished vertex. From a combinatorial point of view, it might not seem to make much difference, but the bijections for pointed maps turn out to be better behaved for probabilistic applications.

bijection, and extend it by an approach reminiscent of [BDG04]. In order to achieve this goal, we somehow fix a local orientation of the surface via a global process, in the sense that the process uses the information of the whole map. As a result, the constraints satisfied by the labels of the encoding objects are also *global* and this provides us from giving a simple characterization of these objects. In the very particular case of quadrangulations, the global constraints can be expressed as local constraints and the encoding objects (so called *well-labeled unicellular maps*) take a simple form and this allowed Chapuy and Dołęga [CD15] to give a combinatorial interpretation of Bender and Canfield's asymptotic formula. In the particular case of triangulations, the same miracle occurs and we are able to give a combinatorial interpretation of the results of [Gao91].

1.2 First definitions

In this work, we work on a compact surface without boundary. Recall that, by the classification theorem, it is either orientable and homeomorphic to the surface obtained by adding h handles to the sphere for some $h \in \{0, 1, \ldots\}$ (sphere, torus, double torus, etc.), or nonorientable and homeomorphic to the surface obtained by adding $2h$ cross-caps to the sphere for some $h \in \{1/2, 1, 3/2, \ldots\}$ (projective plane, Klein bottle, etc.). The number h is called the *type* of the surface.

From now on and until the end of the paper, we fix such a surface $\mathcal{S}$, orientable or not.

A *map* is a cellular embedding of a finite graph (possibly with multiple edges and loops) into $\mathcal{S}$, considered up to homeomorphisms. Cellular means that the *faces* of the map (the connected components of the complement of edges) are homeomorphic to 2-dimensional open disks. Note that, although $\mathcal{S}$ might not be orientable, each face is orientable, so that it will make sense to follow the border of a face, provided a starting orientation is given. A *corner* is an angular sector determined by two consecutive half-edges incident to the same vertex and to the same face. The *degree* of a face is its number of corners. By convention, all the maps we consider are *rooted*, that is, given with a distinguished **oriented** corner called the *root*. It will be represented by a small angular sector with an arrow on the pictures. The (unoriented) corner corresponding to the root will be called the *root corner*, the vertex incident to the root will be called the *root vertex*, the face containing the root will be called the *root face* and the edge incident to the root face that follows the root will be called the *root edge*. See Figure 1.

We will use the following involution we call a *root flip*: from a map $\mathfrak{m}$, we define the root flipped map $\bar{\mathfrak{m}}$ by rerooting $\mathfrak{m}$ at the only oriented corner incident to the other extremity of the root edge and defining the same root edge. We use the classical notation $V(\mathfrak{m})$ to denote the vertex set of a map $\mathfrak{m}$ and we denote by $d_{\mathfrak{m}}$ the graph metric on $V(\mathfrak{m})$. In plain English, $d_{\mathfrak{m}}(u, v)$ is the minimal number of edges one has to cross in order to travel from the vertex u to the vertex v.

An important combinatorial feature a map can have is to be bipartite: a map is *bipartite* if its vertex set can be partitioned into two subsets such that every edge links a vertex from one subset to a vertex from the other subset. Equivalently, a map is bipartite if and only if every cycle made of edges in the map has an even number of edges.

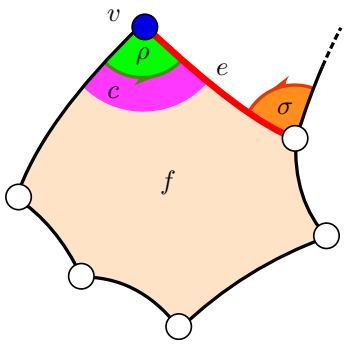

Figure 1: *The (green) root ρ, the (purple) root corner c, the (blue) root vertex v, the (light pink) root face f and the (red) root edge e. The root of the root flipped map is σ (in orange).*

1.3 Aim of the paper

In this work, we present a bijection between the set of pointed bipartite maps on $\mathcal{S}$ and pairs consisting of what we call a *well-labeled unicellular mobile* and a parameter $\varepsilon \in \{+, -\}$. A well-labeled unicellular mobile is a one-face map with green or white vertices whose white vertices carry positive integer labels satisfying some compatibility relations, which need more background to be properly stated (see Definition 2 for a rigorous definition).

If the surface $\mathcal{S}$ is orientable, we recover the famous Bouttier–Di Francesco–Guitter bijection [BDG04] and the following basic properties continue to hold in the nonorientable case (Proposition 4). If $(\mathfrak{m}, v^\bullet)$ is a pointed bipartite map and $((\mathfrak{u}, \mathfrak{l}), \varepsilon)$ denotes the corresponding pair, then

(*i*) $V(\mathfrak{m}) \setminus \{v^\bullet\}$ corresponds to the white vertices of $\mathfrak{u}$ and the label of a white vertex is given by its distance to $v^\bullet$ in $\mathfrak{m}$;

(*ii*) the faces of $\mathfrak{m}$ correspond to the green vertices of $\mathfrak{u}$: moreover, the degree of a face of $\mathfrak{m}$ is twice the degree of the corresponding green vertex;

(*iii*) the maps $\mathfrak{m}$ and $\mathfrak{u}$ have the same number of edges.

Property (*i*) is absolutely crucial from a metric point of view, as the labeled unicellular map somehow captures part of the metric information of the map, namely all the distances to the distinguished vertex $v^\bullet$.

Our construction is based on a rule that gives an orientation to every corner of the map. We introduce what we call *level loops*; these can be thought of as contour lines in topography, where the height of a given vertex is its distance to the distinguished vertex $v^\bullet$. The orientation of the root gives a canonical orientation to all these level loops. Using these local orientations, we then apply similar rules as in the orientable case in order to complete the construction.

We will then see how to extend our bijection to general maps, which are not necessarily bipartite. In the case of triangulations, that is, maps with only faces of degree 3, the encoding mobiles happen to have a particularly simple structure. This allows us to recover the following enumeration result ([Gao91, Theorem 1]; see also [Eyn12]).

Proposition 1. *The number of (rooted) triangulations of $\mathcal{S}$ with $2n$ faces (and thus $3n$ edges and $n+2-2h$ vertices, by the Euler characteristic formula) is asymptotically equivalent to*

$$c_{\mathcal{S}}\, n^{5(h-1)/2}\big(12\sqrt{3}\big)^n\,,$$

where h is the type of $\mathcal{S}$ and $c_{\mathcal{S}}$ is a constant that depends on $\mathcal{S}$.

We will give for $c_{\mathcal{S}}$ a formula involving a summation over cubic maps (Proposition 11). The values for $h \le 1$ are given in Table 1.

orientable			*nonorientable*		
h	$\mathcal{S}$	$c_{\mathcal{S}}$	h	$\mathcal{S}$	$c_{\mathcal{S}}$
0	sphere	$\dfrac{\sqrt{6}}{\sqrt{\pi}}$	$\dfrac{1}{2}$	projective plane	$\dfrac{2^{-3/4}\,3^{5/4}}{\Gamma(3/4)}$
1	torus	$\dfrac{1}{8}$	1	Klein bottle	$\dfrac{3}{2}$

Table 1: *Value of the constant $c_{\mathcal{S}}$ from Proposition 1 for $h \le 1$.*

For small values of h, the generating function of triangulations can also be computed: we recover [Gao91, Theorem 3] and we add the case of the Klein bottle.

Proposition 2. *The generating function of triangulations counted with weight x per vertex is given by*

$$\begin{aligned}
&\frac{1}{2}\sigma^3(1-\sigma)(1-4\sigma+2\sigma^2) && \text{if } \mathcal{S} \text{ is the sphere,}\\
&\frac{1}{2}(1-2\sigma)(1-\sigma+\sigma^2)-\frac{1}{2}\sqrt{1-6\sigma+6\sigma^2} && \text{if } \mathcal{S} \text{ is the projective plane,}\\
&\frac{1}{2}\sigma(1-\sigma)\big(1-6\sigma+6\sigma^2\big)^{-2} && \text{if } \mathcal{S} \text{ is the torus,}
\end{aligned}$$

and

$$3\sigma(1-\sigma)\big(1-6\sigma+6\sigma^2\big)^{-2}\Big(7-30\sigma+30\sigma^2-6(1-2\sigma)\sqrt{1-6\sigma+6\sigma^2}\Big)$$

if $\mathcal{S}$ is the Klein bottle, where σ is an algebraic function of x given by

$$x=\frac{1}{2}\sigma(1-\sigma)(1-2\sigma)\qquad \sigma(0)=0.$$

In the orientable case, our bijection is the already known Bouttier–Di Francesco–Guitter bijection and Propositions 1 and 2 are obtained by the method we use without needing our general bijection. As we did not find this in the literature, even in the easy case of the sphere, we fully treat it here. Note however that, in the case of the sphere, a computation that is similar in spirit was done in [BDG02] and, in the orientable case, Chapuy [Cha09] used the same method in order to obtain similar formulas for maps with face degrees belonging to a given subset of $2\mathbb{N}$ (he also derived results in the more general context of m-constellations and m-hypermaps). Finally, the

analog of Proposition 1 was obtained by the same method for quadrangulations on an orientable surface in [CMS09], as well as on a nonorientable surface in [CD15].

Unfortunately, the constraints on the labels of a well-labeled unicellular mobile in general are too intricate to derive similar enumeration results. In fact, the labels satisfy *global* constraints instead of just *local* constraints as soon as the maps we consider are neither triangulations nor quadrangulations.

The remaining of the paper is organized as follows. We start in Section 2 by presenting the simpler case of bipartite quadrangulations. Rather than using the presentation of [CD15], we use a simplified version of our general framework: this will serve as a warm-up for the general case. There will be no proof in this section as it is a special case (Corollary 7) of our more general bijection. Section 3 is devoted to the bijection for bipartite maps and we then extend the bijection to general maps in Section 4, focusing on the particular case of triangulations in Section 4.2. Finally, in Annex A, we give alternate figures using the useful representation of a unicellular map as a polygon with paired sides.

Acknowledgements. This work is partially supported by Grant ANR-14-CE25-0014 (GRAAL). The author also acknowledges partial support from the Isaac Newton Institute for Mathematical Sciences where part of this work was conducted. We thank Guillaume Chapuy and Maciej Dołęga for stimulating discussions and for sharing their paper [CD15] with us, as well as Grégory Miermont for encouraging discussions, especially about further developments on the subject of nonorientable Brownian surfaces. Finally, we thank Élie de Panafieu and Emmanuel Guitter for discussions on the enumeration application.

2 The case of bipartite quadrangulations

Before presenting our bijection for general bipartite maps, let us first focus on bipartite quadrangulations. Recall that a quadrangulation is a map with only faces of degree 4 (see Figure 2).

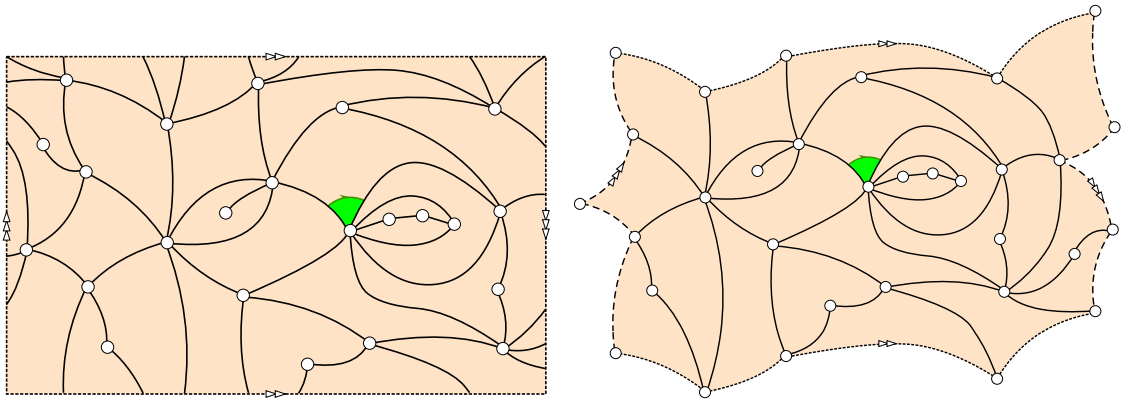

Figure 2: *A bipartite quadrangulation on the Klein bottle with 23 faces. The root is symbolized by the green arrowhead. On the right, the elementary domain has been chosen in order better to fit the map.*

The first bijection of the kind considered in this paper focused on (necessarily bipartite) quadrangulations of the sphere and was introduced by Cori and Vauquelin [CV81] and later popularized by Schaeffer [Sch98]. It was then generalized by Chapuy, Marcus and Schaeffer [CMS09] to orientable bipartite quadrangulations and later by Chapuy and Dołęga [CD15] to nonorientable bipartite quadrangulations. We now present the latter bijection, which contains all the previous ones as specializations. We use a rather different presentation than in [CD15], which will be more suited for our generalization: in particular, we introduce the notion of *level loop*, which replaces the notion of dual exploration graph used in [CD15]. Moreover, our presentation has the advantage of providing an explicit construction for pointed quadrangulations.

2.1 From pointed bipartite quadrangulations to well-labeled unicellular maps

We start from a pointed bipartite quadrangulation $(\mathfrak{q}, v^\bullet)$ and we define the labeling function $\mathfrak{l} : V(\mathfrak{q}) \to \mathbb{Z}_+$ by

$$\mathfrak{l}(v) := d_{\mathfrak{q}}(v^\bullet, v), \qquad v \in V(\mathfrak{q}).$$

Note that, as the quadrangulation is bipartite, the labels of two neighboring vertices differ by exactly 1. If the root vertex has a smaller label than the other extremity of the root edge, we set $\varepsilon := +$. Otherwise, we replace $\mathfrak{q}$ by its root flipped version $\bar{\mathfrak{q}}$ and set $\varepsilon := -$. The first step of the construction somehow defines a canonical local orientation of the map thanks to oriented level loops, which we now explain how to construct.

At this stage, we only construct *unoriented* level loops: we will orient all the loops at the end. We start from a corner incident to $v^\bullet$ and we move along the side of an incident edge (necessarily visited from label 0 to 1). We then turn around the vertex labeled 1, crossing edges linking it to vertices labeled 2 until we reach an edge linking it to a vertex labeled 0. We then move along the side of this edge and reach a corner with label 0. We move along the side of the first subsequent edge and iterate this process until we come back to the initial corner and close the loop. This loop visits some corners of type 1-0-1 (corners incident to a vertex with label 0 and such that the two incident edges link it to vertices labeled 1), as well as some corners of type 2-1-2. If there are still corners of type 1-0-1 not visited by the loop, we construct the next loop by the same process, starting from an unvisited corner and we iterate the process until all corners incident to $v^\bullet$ have been visited. We say that the level loops we have created so far are at *level* 1. See Figure 3.

We consider the corners of type 2-1-2 and construct the level loops at level 2 by the same method, following vertices alternatively labeled 1 and 2 and crossing edges linking vertices with labels 2 and 3. We then iterate the process with every corner of type $i+1$-i-$i+1$ for some i and construct all the (unoriented) level loops. The loops starting from corners of type $i+1$-i-$i+1$ (and visiting corners of type $i+1$-i-$i+1$ or $i+2$-$i+1$-$i+2$) are said to be at level $i+1$.

We now use the root of the quadrangulation in order to orient, give an origin and order the level loops we created. Before proceeding, we add around $v^\bullet$ a single loop at level 0. If the root corner is visited by exactly one loop, we declare this loop to be the first loop, we set its origin at the root corner and we orient it by the orientation given by the root. Otherwise, by construction, there are exactly two such loops, we declare the one at lower level to be the first one and the one at higher level to be the second one. We set their origin and orientation as before.

We start from the origin of the first loop and travel on it. Every time we encounter a new loop (in the sense that we visit a corner that is also visited by another loop that has not yet been oriented), we declare it to be the next one in the order we are creating. We also set its origin at the

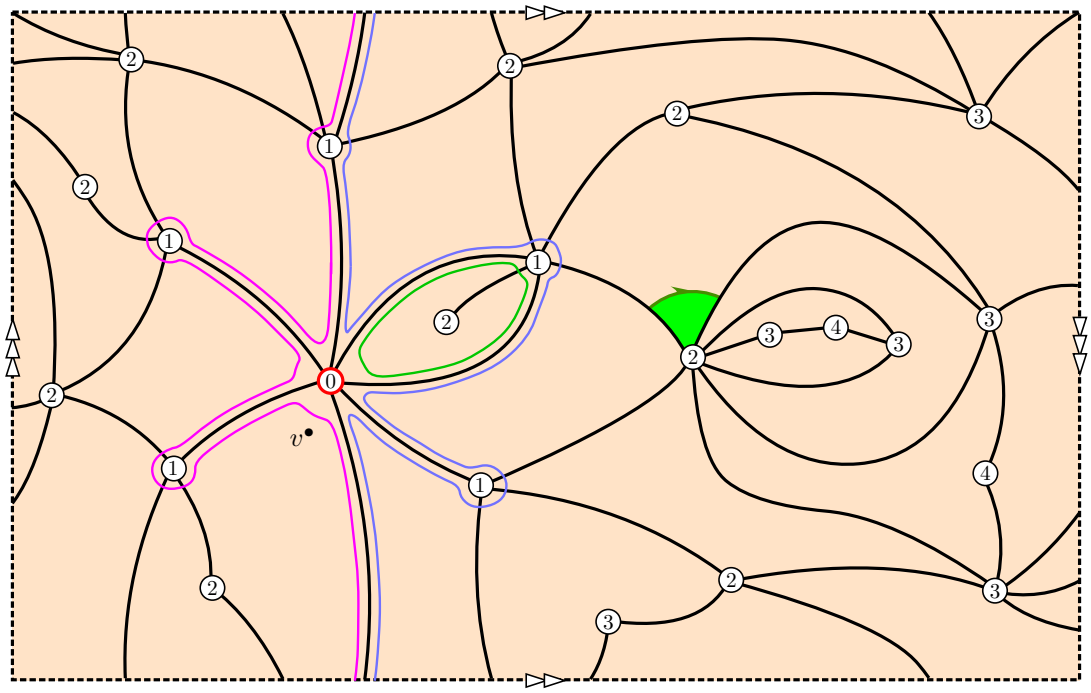

Figure 3: *The (unoriented) level loops at level* 1.

location we are and we orient it by the orientation induced by the loop on which we are traveling. When we arrive back at the origin of our loop, we move to the next one and iterate the process until every loop has been oriented. See Figure 4.

Remark. If the surface we consider is orientable, all the loops are merely oriented according to the orientation of the surface induced by the orientation of the root. This orientation step may thus be circumvented and this explains why it was not present in the previously cited works that focus on orientable surfaces.

We may now finish the construction. In each face, we add an extra edge (in green on the figures) as follows. If the labels of the corners of the face are i, $i+1$, i, $i+1$, we link the two corners with label $i+1$. If the labels are i, $i+1$, $i+2$, $i+1$, there is a level loop at level $i+1$ that enters the face, visits a corner with label $i+1$ then the corner with label i and finally the other corner with label $i+1$ before exiting the face. We link the **last** corner with label $i+1$ visited by this loop to the corner with label $i+2$. We then consider the embedded graph $\mathfrak{u}$ with vertex set $V(\mathfrak{q}) \setminus \{v^\bullet\}$ and edge set the set of green edges we added. We root it as follows. We first consider the root edge of $\mathfrak{q}$ and we select its half-edge that is not incident to the root vertex. This half-edge corresponds to one corner of $\mathfrak{u}$, which we declare to be the root corner of $\mathfrak{u}$. Finally, the orientation of the root of $\mathfrak{q}$ gives a canonical orientation to the half-edge we selected and thus to the root corner of $\mathfrak{u}$ (see Figure 5). The vertices of $\mathfrak{u}$ are moreover naturally labeled by the function $\mathfrak{l}$.

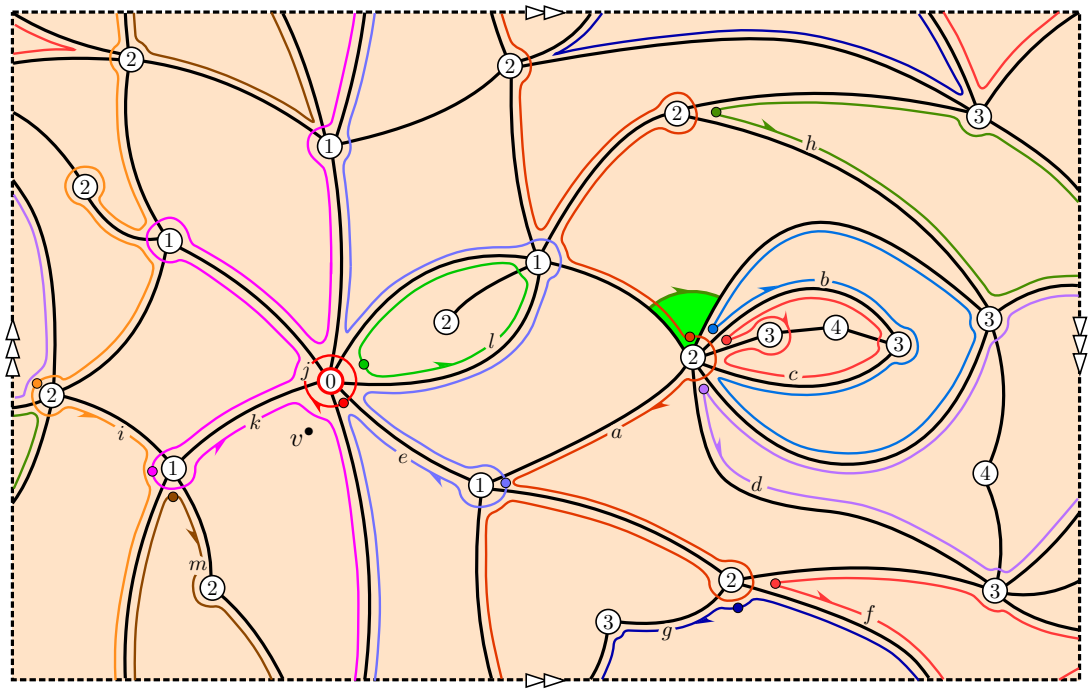

Figure 4: *All the level loops. The letters indicate their rank in the order, the half-arrowheads their orientation and the dots their origin. Loop j is at level 0, loops e, k and l are at level 1, loops a, i and m are at level 2 and the remaining loops are at level 3.*

The object $(\mathfrak{u}, \mathfrak{l})$ we obtain is a *well-labeled unicellular map*, meaning that $\mathfrak{u}$ is a rooted one-face map of $\mathcal{S}$ and $\mathfrak{l} : V(\mathfrak{u}) \to \mathbb{N}$ is a function with minimum 1 and such that $\mathfrak{l}(u) - \mathfrak{l}(v) \in \{-1, 0, 1\}$ for every pair (u, v) of neighboring vertices. See Figure 6.

2.2 From well-labeled unicellular maps to pointed bipartite quadrangulations

The inverse mapping constructs a pointed quadrangulation from a well-labeled unicellular map $(\mathfrak{u}, \mathfrak{l})$ and a parameter $\varepsilon \in \{+, -\}$ as follows. We first add inside the unique face of $\mathfrak{u}$ a new vertex $v^\bullet$ and assign to it the label $\mathfrak{l}(v^\bullet) := 0$. We connect all the corners with label 1 to this vertex $v^\bullet$ in a noncrossing fashion. We thus create a certain number of *sectors*, defined as the connected components of the complement of the newly added edges and the original edges of $\mathfrak{u}$. The set of corners of $\mathfrak{u}$ belonging to a sector is called the *arc* of the sector and the remaining corner of the sector is called its *inner corner*.

Inside each sector whose arc contains at least three corners, we add a temporary vertex to which we connect all the corners with label 2 (note that the first and last corners in such a sector are labeled 1 by definition and the second and second to last are necessarily labeled 2). The added edges delimit new sectors, defined as the connected components that do not contain the inner corner of the original sector. We iterate the construction inside each created sector. The *level* of a

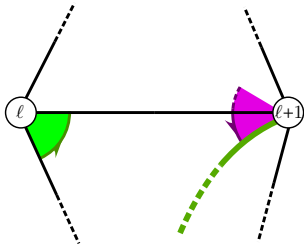

Figure 5: *Rooting* $\mathfrak{u}$ *from the root of* $\mathfrak{q}$*. The root of* $\mathfrak{q}$ *is represented in green and the root of* $\mathfrak{u}$ *is in purple. The existence of the green edge (of* $\mathfrak{u}$*) is ensured by the rules of the construction.*

sector is the minimal label of the corners on its arc (attained only once at each extremity of the arc, by definition).

We then construct the unoriented level loops. We start from the inner corner of a sector and we move along one of the two edges linking it to a corner of $\mathfrak{u}$. When we reach an edge of $\mathfrak{u}$, we cross it and continue to move along the new edge we meet, toward the inner corner of the sector we visit. When we reach the inner corner, we move along the side of the other edge linking it to a corner of $\mathfrak{u}$ and we iterate the process until we close the loop. We then select an inner corner that has not been visited by the loop and iterate the process until all the inner corners have been visited by a loop. See Figure 7 (or 21 for another representation). The *level* of a loop is the common level of the sectors it visits. We also add around $v^\bullet$ a single loop at level 0.

Before orienting the loops, we need to find the future root of the quadrangulation. We consider the added edge linking the root vertex of $\mathfrak{u}$ to $v^\bullet$ or to a temporary vertex and we select its half-edge that is not incident to the root vertex of $\mathfrak{u}$. The root of $\mathfrak{u}$ gives a canonical orientation to this half-edge and the future root of $\mathfrak{q}$ is the oriented corner preceding this half-edge in this orientation, as depicted on Figure 8.

We now orient, give an origin and order the level loops. In the same time, we also identify the temporary vertices with some vertices of $\mathfrak{u}$. More precisely, every time we orient a loop, inside each sector it visits, we identify the temporary vertex of the subsectors at next level with the first vertex of the sector that is visited by the portion of the level loop inside the sector. We consider the sector at higher level that contains the future root and we orient the loop visiting its inner corner in such a way that its orientation around $v^\bullet$ is prescribed by the orientation of the future root. We do the aforementioned identifications.

Two cases may happen.

(*a*) If the future root corner is not an inner corner and is visited by a loop, we set this loop to be the first loop and we set its origin at the future root corner. Note that this loop is the loop we just oriented.

(*b*) If the future root corner is an inner corner, we orient the loop visiting the sector at previous level containing the sector we consider and set this loop to be the first one. The loop we oriented before is set to be the second one. With the identifications resulting of the orientation of the first loop, the two loops visit the future root corner and we set their origin at this corner.

We start from the origin of the first loop and travel on it. Every time we visit a temporary

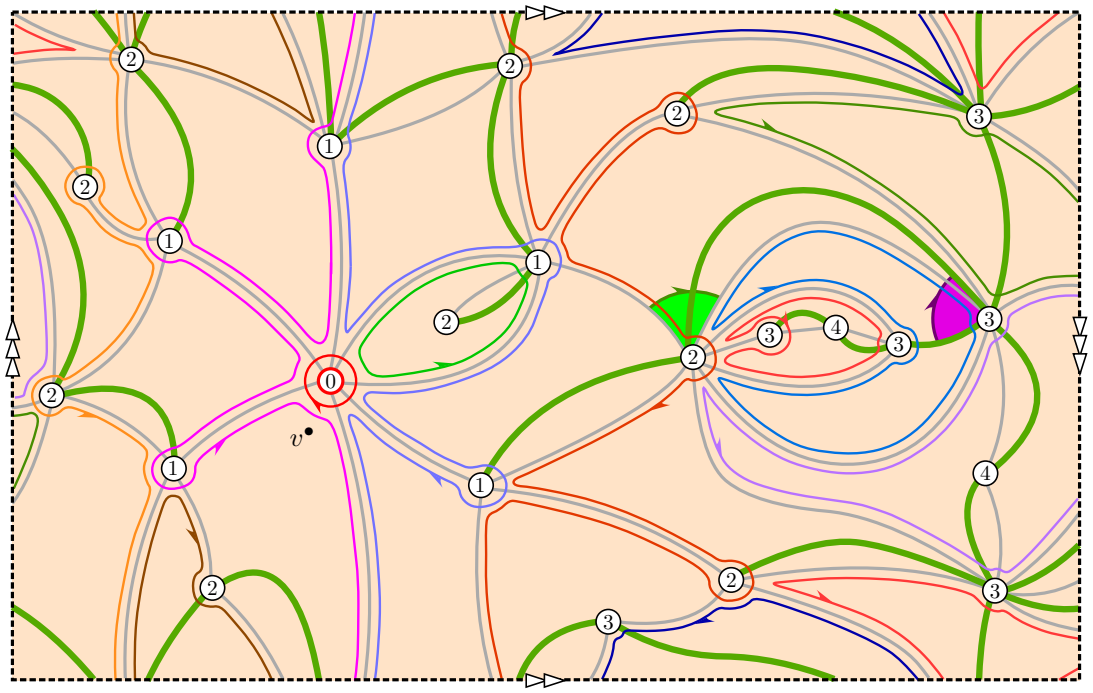

Figure 6: *The Chapuy–Dołęga bijection, from a pointed bipartite quadrangulation to a well-labeled unicellular map. The edges of the original quadrangulation have been grayed out.*

vertex that has not been identified, we orient the loop visiting the sector at previous level in the same orientation as the orientation of the loop on which we are traveling. We declare this loop to be the next one and we set its origin at the location we are. Similarly, every time we visit an inner corner and see a new loop, we declare it to be the next one, we set its origin at the location we are and we orient it by the orientation induced by the loop on which we are traveling. When we arrive back at the origin of our loop, we move to the next one and iterate the process until every loop has been oriented. See Figures 9 and 22.

The embedded graph $\mathfrak{q}$ made of the added edges and rooted at the future root is a bipartite quadrangulation. If $\varepsilon = +$, then the output of the construction is $(\mathfrak{q}, v^\bullet)$ and if $\varepsilon = -$, then the output is the root flipped version $(\bar{\mathfrak{q}}, v^\bullet)$. This construction is the inverse of the one from Section 2.1.

2.3 Other choices of orientations, other bijections

In the previous construction, we had the opportunity to choose the orientation of every loop and we decided to use, by default, the orientation induced by the root or by the loop we were visiting. We can modify this rule as follows. We fix beforehand a sequence of rules "$+$" or "$-$" and, every time we orient a new loop, we reverse its orientation if and only if the current rule is "$-$."

For every choice of sequence, we obtain a different pair of mappings, which are inverse one from another. In fact, any loop orientation process of that is tractable will provide a bijection.

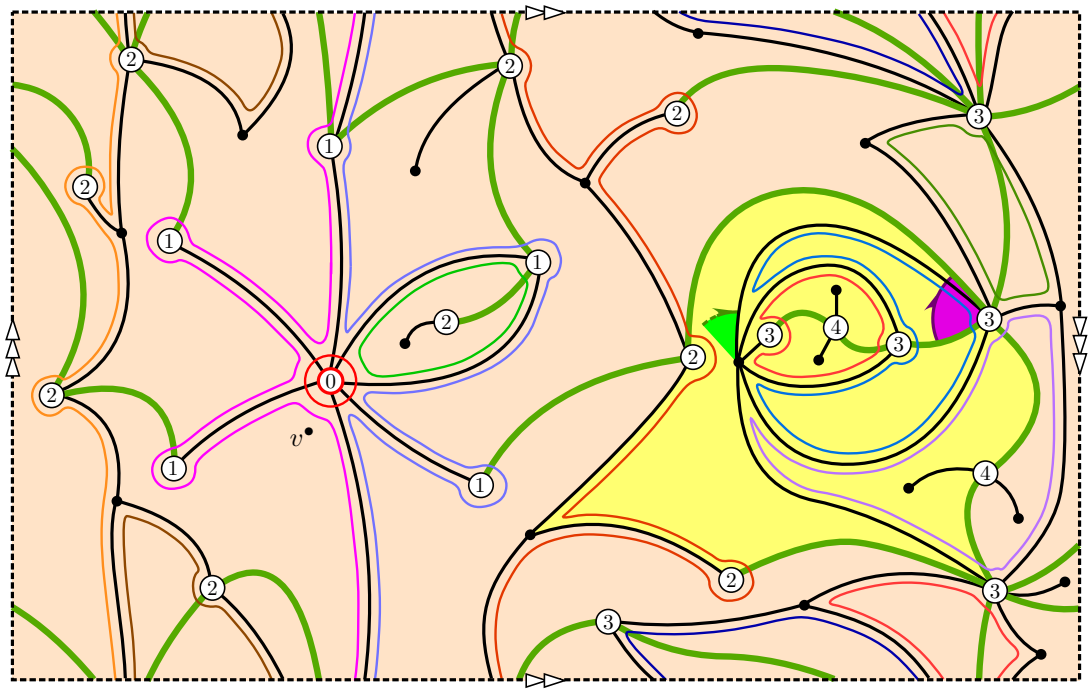

Figure 7: *The sectors and unoriented level loops. The future root is represented and the sector at level* 2 *containing it is highlighted.*

3 The mappings for bipartite maps

Let us now turn to general maps. The construction we give here is a generalization of the Bouttier–Di Francesco–Guitter bijection [BDG04] for general orientable maps and of the construction presented in the previous section. We start with the simpler case of bipartite maps in this section.

3.1 From pointed bipartite maps to well-labeled unicellular mobiles

Let $(\mathfrak{m}, v^\bullet)$ be a pointed bipartite map. As before, we define the labeling function $\mathfrak{l} : V(\mathfrak{m}) \to \mathbb{Z}_+$ by

$$\mathfrak{l}(v) := d_{\mathfrak{m}}(v^\bullet, v), \qquad v \in V(\mathfrak{m}).$$

Here again, the fact that $\mathfrak{m}$ is bipartite implies that the labels of two neighboring vertices differ by exactly 1. If the root vertex has a smaller label than the other extremity of the root edge, we set $\varepsilon := +$; otherwise, we replace $\mathfrak{m}$ by its root flipped version $\bar{\mathfrak{m}}$ and set $\varepsilon := -$. We generalize the construction of level loops as follows. We consider the border of a face along some edge and we denote by $i-1$ and i the labels of the vertices incident to this edge. We travel on the border of the face along the edge, from the vertex labeled $i-1$ toward the vertex labeled i. When we reach the vertex labeled i, we turn around the vertex until we see an edge linking it to a vertex with label $i-1$; in the process, we cross a nonnegative number of edges linking the vertex to vertices labeled $i+1$. We then travel along the edge toward the vertex labeled $i-1$. We keep traveling along the

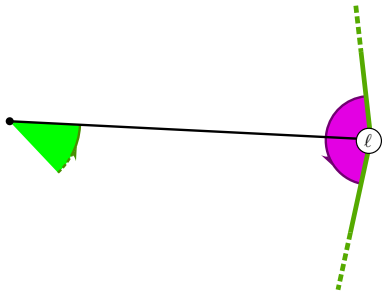

Figure 8: *The future root of* $\mathfrak{q}$ *(in green) from the root of* $\mathfrak{u}$ *(in purple).*

border of the face we are visiting until we either close the loop or reach a vertex labeled $i+1$. In the later case, the vertex visited just before the vertex labeled $i+1$ necessarily has label i; we turn around this vertex until we see an edge linking it to a vertex with label $i-1$. We iterate the process until we close the loop. We say that such a loop is at level i. We iterate the process until each side of every edge of type $i-1$ - i is visited by a loop at level i. We finally add around $v^\bullet$ a single loop at level 0.

Remark. For a quadrangulation, the loops are the same as in Section 2, with the addition of a single loop at level $i+2$ inside each face of type i - $i+1$ - $i+2$ - $i+1$.

We orient, give an origin and order the level loops as follows. We consider all the loops visiting the root corner: note that there exists at least one such loop. We orient all these loops according to the orientation given by the root, we set their origin at the root corner and we declare them to be the first loops, ordered by increasing level. We then start from the origin of the first loop and travel on it. Every time we encounter new loops, we declare them to be the next ones, ordered in increasing level. We set their origin at the location we are and we orient them by the orientation induced by the loop on which we are traveling. When we arrive back at the origin of our loop, we move to the next one and iterate the process until every loop has been oriented. See Figure 10. Note that this operation terminates as every loop at level $i \geq 1$ touches a loop at level $i-1$. Indeed, we constructed the loop at level i by starting from the side of an edge of type $i-1$ - i. If $i=1$, the corner labeled $i-1$ is visited by the single loop at level 0. If $i>1$, considering the two edges of type $i-2$ - $i-1$ before and after this corner around the incident vertex, we see that a loop at level $i-1$ has to pass through it.

We consider a loop and denote by i its level. The loop visits one by one several corners of the map. Among these corners, we say that the loop *selects* those with label i that are immediately preceded by a corner labeled $i-1$. In other words, if the loop is not completely included in a face, for every face it visits, it selects all the corners labeled i it visits, except for the first corner of the face. If the loop is completely included in a face, it is a loop at maximal level and it visits every corner of the face: its thus selects all the corners whose label is maximal among the labels of the vertices incident to the face.

We add an extra vertex in the middle of every face: these vertices will be called *green vertices* in the following, in contrast with the original vertices, which we will call *white vertices*. Inside each face, we link in a noncrossing fashion by *green edges* all the corners that are selected by some loop to the green vertex of the face.

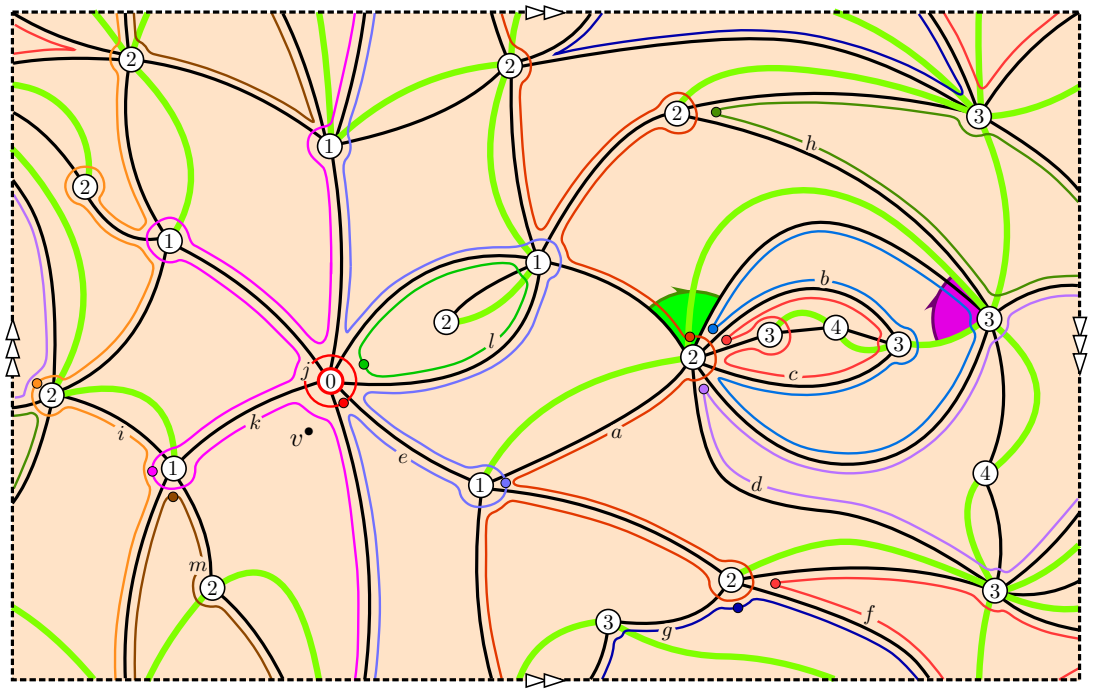

Figure 9: *The Chapuy–Dołęga bijection, from a well-labeled unicellular map to a pointed bipartite quadrangulation. Note that everything was done in such a way that the level loops correspond through the bijection.*

Finally, we consider the embedded graph $\mathfrak{u}$ whose vertex set consists of the union of $V_\circ(\mathfrak{u}) := V(\mathfrak{m}) \setminus \{v^\bullet\}$ with the set $V_\bullet(\mathfrak{u})$ of green vertices and whose edge set is composed of the green edges. We root it with the convention depicted on Figure 5. The white vertices of $\mathfrak{u}$ inherit the labels from the function $\mathfrak{l}$: we set $\Phi(\mathfrak{m}, v^\bullet) := ((\mathfrak{u}, \mathfrak{l}), \varepsilon)$. See Figure 11.

3.2 Definition of the encoding object and inverse construction

3.2.1 Preliminaries

We now describe in more details the encoding object we obtained in Section 3.1. First, we say that a pair $(\mathfrak{u}, \mathfrak{l})$ is a *labeled unicellular mobile* if it satisfies the following conditions:

- $\mathfrak{u}$ is a rooted one-face map of $\mathcal{S}$ whose vertex set is partitioned into $V_\bullet(\mathfrak{u}) \sqcup V_\circ(\mathfrak{u})$ in such a way that every edge links a vertex from $V_\bullet(\mathfrak{u})$ to a vertex from $V_\circ(\mathfrak{u})$;
- $\mathfrak{l} : V_\circ(\mathfrak{u}) \to \mathbb{N}$ is a function with minimum 1;
- the root vertex belongs to $V_\circ(\mathfrak{u})$.

As the face of $\mathfrak{u}$ is homeomorphic to a disk by definition, and as the root of $\mathfrak{u}$ gives a canonical orientation to this disk, the corners of $\mathfrak{u}$ are naturally ordered in a cyclic way around its face. In what follows, we only consider the corners of $\mathfrak{u}$ that are incident to vertices of $V_\circ(\mathfrak{u})$.

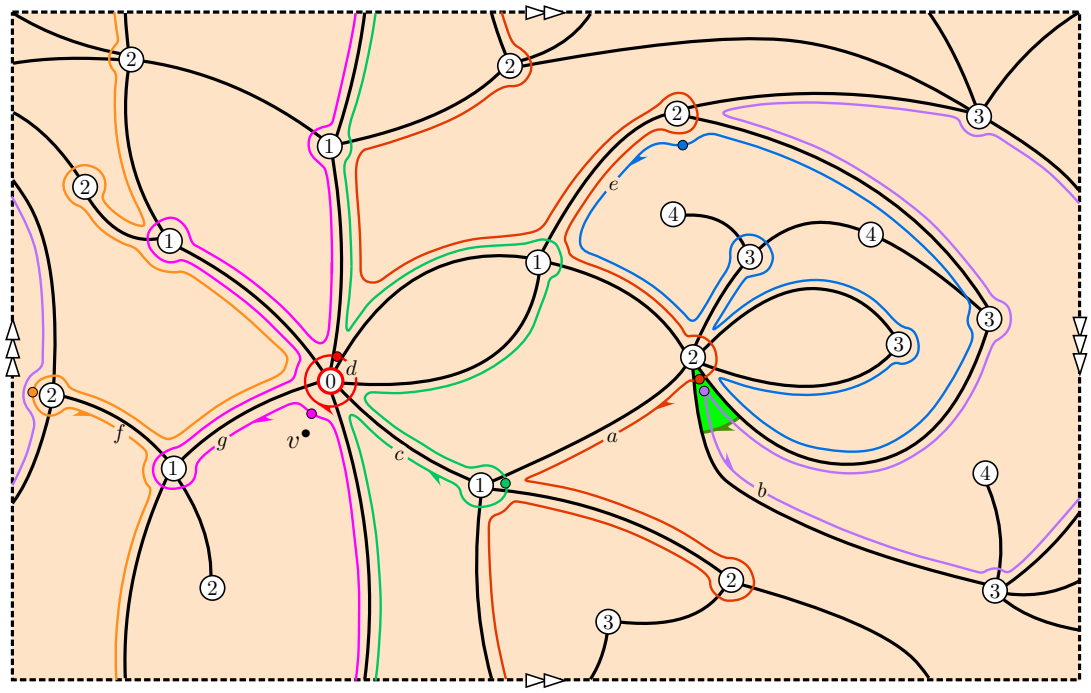

Figure 10: *The level loops for a bipartite map. Inside each face, the single loop at maximal level is not represented and not taken into account in the ordering of the loops: on this example, the presence of these maximal loops does not affect the relative order of the other loops.*

Definition 1. *We call* arc *any contiguous interval of two or more subsequent corners such that the first and last corners have strictly smaller labels than the other corners. The first and last corners of the arc are called its* extremities *and the other corners are called its* internal corners.

An arc whose extremities have labels i and j is called an $\{i, j\}$-arc and its level is defined as the number $i \vee j$. An arc is said to be trivial *if it contains only two corners.*

Lemma 3. *We have the following properties.*

(i) Let A and B be two distinct nontrivial arcs whose intersection contains internal corners of A or B. Then $A \subseteq B$ or $B \subseteq A$. Moreover, the level of the larger arc is strictly lower than the level of the smaller arc.

(ii) The following properties are equivalent:

(a) For all $i \geq 1$, every nontrivial arc at level i contains a corner with label $i + 1$.

(b) For all $i \geq 1$, every nontrivial arc at level i has a range of internal corner labels of the form $\{i + 1, i + 2, \ldots, m\}$ for some m.

(c) For all $i \geq 2$ and for every corner with label i, either the first subsequent corner with label strictly smaller than i has label $i - 1$ or the last preceding corner with label strictly smaller than i has label $i - 1$.

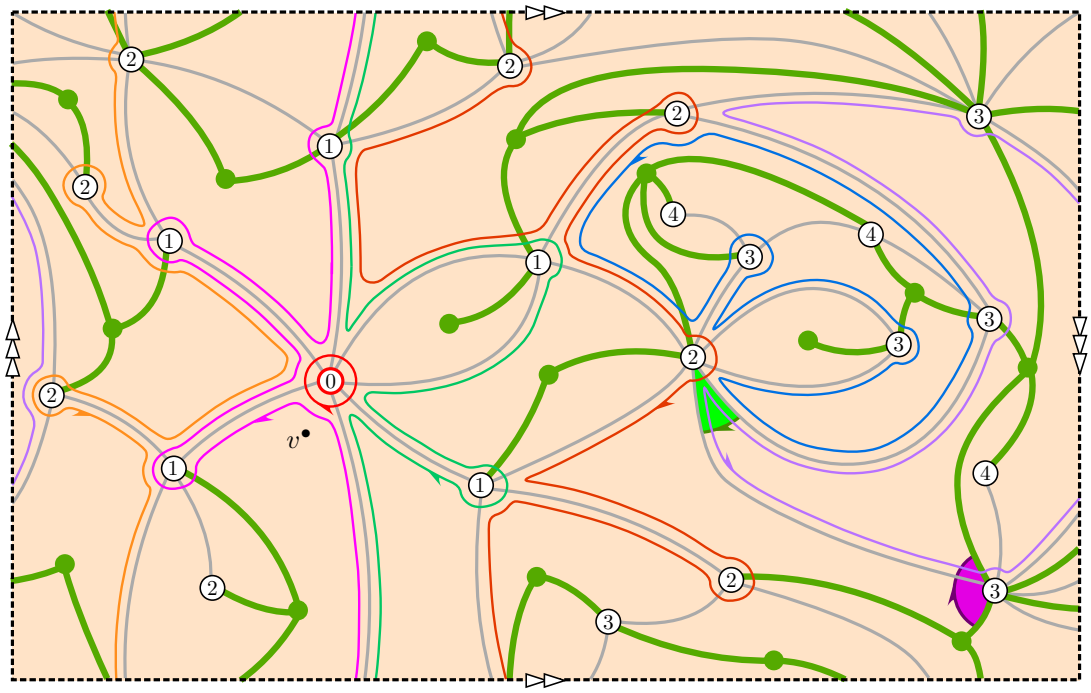

Figure 11: *The bijection, from a pointed bipartite map to a well-labeled unicellular mobile. The edges of the original map have been grayed out.*

(iii) The properties of (ii) imply that, for all $i \geq 2$, every arc at level $i \geq 2$ is included in a unique arc at level $i-1$, which is nontrivial. Similarly, every corner labeled $i \geq 2$ is included in a unique arc at level $i-1$, which is nontrivial.

Proof. (*i*) Let us argue by contradiction and suppose that A and B satisfy the hypotheses but not the conclusion. Denoting by a, a' the extremities of A and by b, b' the extremities of B, we may suppose without loss of generality that $a < b < a' \leq b'$ in the cyclic order around the face of $\mathfrak{u}$. Then we must have $\mathfrak{l}(a') < \mathfrak{l}(b)$ as A is an arc and $\mathfrak{l}(a') > \mathfrak{l}(b)$ as B is an arc. This is a contradiction.

As the smaller arc has an extremity that is an internal corner of the larger arc, its level is larger the label of this extremity, which is strictly larger than the level of the larger arc.

(*ii*) Let us suppose (*a*) and show (*b*). We take a nontrivial arc A at level i and denote by m the maximum label of its internal corners. If $m = i+1$, we are done. Otherwise, we select a corner c with label m and denote by a and b the extremities of A. We denote by a' the last corner of A before c with label less than or equal to $i+1$ and by b' the first corner after c with label less than or equal to $i+1$. By (*a*), at least one of the corners a', b' has label $i+1$. We replace A by the arc with extremities a' and b' and iterate the argument.

Let us suppose (*b*) and show (*c*). We consider a corner with label i and denote by a (resp. b) the last preceding corner (resp. the first subsequent corner) with label strictly smaller than i. Then the interval with extremities a and b is an arc. By definition, the minimal label of its internal corners is i so its level must be $i-1$ by (*b*) and thus $\mathfrak{l}(a) \vee \mathfrak{l}(b) = i-1$.

Let us suppose (*c*). We consider a nontrivial arc at level i and denote by j the minimal label of its internal corners. We apply (*c*) to an internal corner with label j and obtain that the maximal label of the extremities of the arc is $j-1$. But this label is i by definition of the level, so that (*a*) holds.

(*iii*) Let A be an arc at level i with extremities a and a'. Let b be the last corner preceding a in the large sense with label strictly smaller than i and let b' be the first subsequent corner after a' in the large sense with label strictly smaller than i. Then the arc B with extremities b and b' that contains A is at level $i-1$ by (*ii*)(*c*). It is nontrivial as it contains at least a, a', b and b' and $(b,b') \neq (a,a')$. By (*i*), it is the only arc with the required properties. The second property is shown similarly, by replacing a and a' with the considered corner and observing that, in this case, both b and b' differ from the considered corner. □

3.2.2 Construction

In order to give the explicit conditions satisfied by a well-labeled unicellular mobile, we need to start performing the inverse construction. We suppose that $(\mathfrak{u}, \mathfrak{l})$ is a labeled unicellular mobile satisfying the properties of Lemma 3.(*ii*). We add inside the unique face of $\mathfrak{u}$ a new vertex $v^\bullet$ with label $\mathfrak{l}(v^\bullet) := 0$. We connect all the corners with label 1 to $v^\bullet$ in a noncrossing fashion and, for each nontrivial arc at level $i \geq 2$, we add a temporary vertex to which we link all its corners that are labeled $i+1$. Note that Lemma 3.(*i*) ensures that this can be done in a noncrossing fashion.

We now construct the unoriented level loops. Notice that, by Lemma 3.(*iii*), every corner of $\mathfrak{u}$ is linked either to $v^\bullet$ or to a temporary vertex. We call *black edges* these links. We select a corner of $\mathfrak{u}$ and one incident edge of $\mathfrak{u}$. We denote by i the label of the selected corner. Starting from the selected corner, we explore the boundary of the face of $\mathfrak{u}$, in the orientation given by the selected edge. We search the first subsequent corner with label smaller than or equal to i. We then begin to draw a loop from the selected corner to the second one, without crossing black edges; this can be done as two corners of $\mathfrak{u}$ are linked to the same temporary vertex if and only if they have the same label and all the corners in one of the two intervals they delimit have labels larger than or equal to this common label. We then cross the edge of $\mathfrak{u}$ at the second corner and iterate the process (always with the same i) until we close the loop. We thus create a loop and define its level to be i. We iterate the process until every side of every black edge starting from a corner labeled i is visited by a loop at level i. We finally add a single loop at level 0 around $v^\bullet$. See Figure 12 or Figure 23.

By construction, every portion of loop included in the face of $\mathfrak{u}$ delimits an arc of $(\mathfrak{u}, \mathfrak{l})$. More precisely, every arc delimited by a portion of loop at level i is either trivial at level less than or equal to i or nontrivial at level i. Indeed, if such an arc is a $\{j,k\}$-arc, we have $j \leq i$ and $k \leq i$ by construction and, if it is moreover nontrivial, every internal corner has label strictly larger than i, so that the level is at least i, by Lemma 3.(*ii*)(*b*). Moreover, every nontrivial arc is delimited by exactly one loop and every trivial arc is delimited by at least one loop. We say that a level loop at level i is *well oriented* if every nontrivial arc it delimits is such that the extremity first visited by the portion of loop inside the face of $\mathfrak{u}$ has label i. Note that, in general, it is possible that no orientations, exactly one orientation or both orientations of an unoriented level loop yield a well-oriented level loop.

Let A be an arc at level $i \geq 2$ and let B be the arc at level $i-1$ defined by Lemma 3.(*iii*). As B is nontrivial, there is a unique loop that delimits it. We say that this loop *overflies* the portions of loops delimiting A (there may be more than one portion if A is trivial). We also say that the portions of

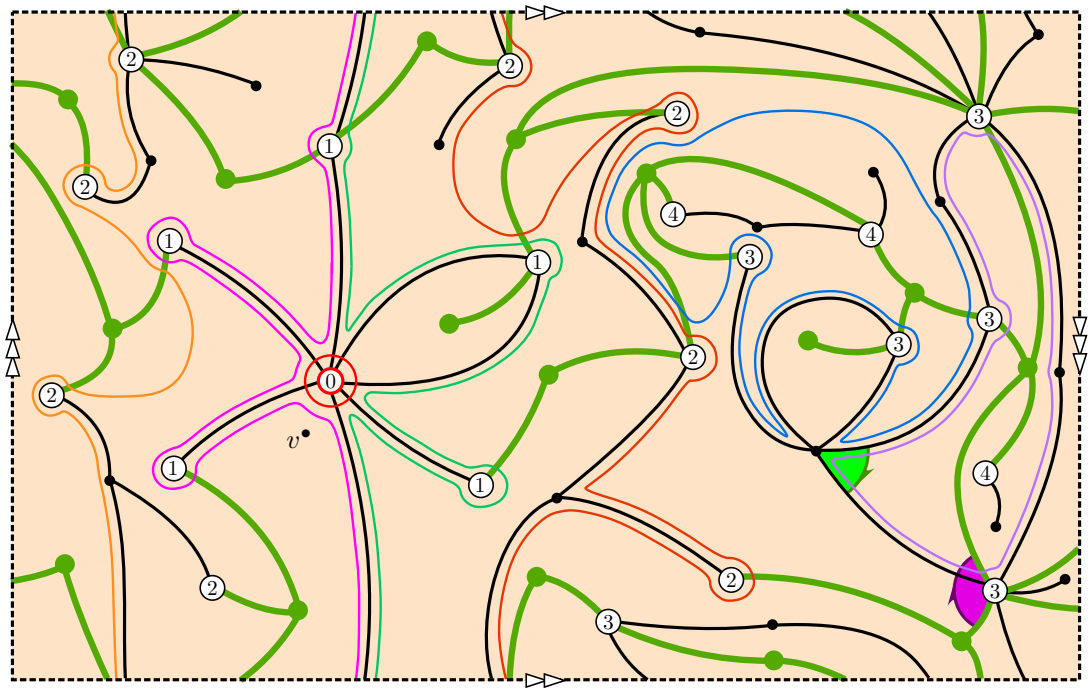

Figure 12: *The unoriented level loops. Here again, we did not represent the loops at maximal level, that is, the loops circling around a single green vertex.*

loops delimiting the arcs at level 1 are overflown by the single loop at level 0. We similarly define the loop overflying a corner.

We use the same method as in the case of quadrangulations in order to define the future root of the map, shown on Figure 8. Using this future root, we will orient, give an origin and order a few level loops. Every time we orient a loop, we do the following. If the loop is not well oriented, we stop the process. If the loop is well oriented, for each nontrivial arc it delimits, we identify the corresponding temporary vertex with the extremity of the arc that is first visited by the portion of loop inside the face of $\mathfrak{u}$. By Lemma 3.(*i*), this operation can be done in such a way that the black edges do not cross each other. Let us consider such a nontrivial $\{i, j\}$-arc, where $i \geq j$ is the common level of the arc and of the loop. Denoting by $k \geq 1$ the number of corners labeled $i + 1$ in this arc, we see that the arc is split into $k + 1$ subarcs at level $i + 1$, namely one $\{i, i + 1\}$-arc, $k - 1$ $\{i + 1, i + 1\}$-arcs and one $\{i + 1, j\}$-arc. When we travel on the portion of loop corresponding to the arc, we first "see" the other loops crossing the same first edge of $\mathfrak{u}$, then the loops delimiting the $k - 1$ $\{i + 1, i + 1\}$-arcs, then the loops delimiting the $\{i + 1, j\}$-arc, then the loop that overflies the portion we visit and finally the loops that cross the same last edge of $\mathfrak{u}$. See Figure 13.

The first loop in our order is the loop overflying the root corner of $\mathfrak{u}$. We orient it by the orientation prescribed by the future root and do the aforementioned identifications (provided that it is well oriented). After these identifications, the first loop passes through the future root corner. We set its origin at this location. We then travel on the first loop, starting at its origin. Every time

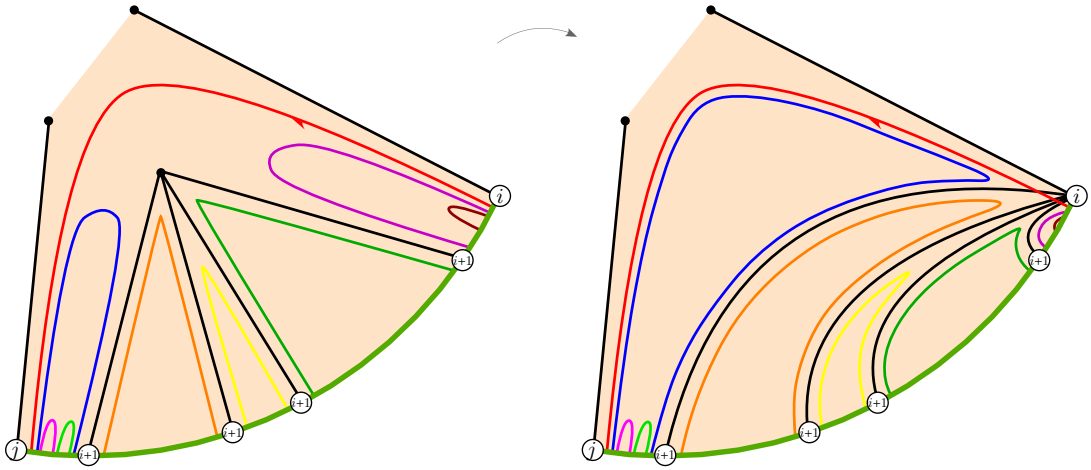

Figure 13: *Identification of a temporary vertex. The red loop delimits the $\{i, j\}$-arc ($i \geq j$) and the temporary vertex corresponding to this arc is identified with the first extremity visited by the portion of loop. When traveling on the red loop, we "see" the other loops in the order brown, purple, green, yellow, orange, blue, then the overflying loop (not represented) and finally light green and light purple.*

we see an unoriented loop, we orient it in the same orientation as the orientation of the loop on which we are traveling. We declare this loop to be the next one and we set its origin at the location we are. If we see several new loops at the same time, we order them by increasing level. When we arrive back at the origin of our loop, we move to the next one and iterate the process until either we create a loop that is not well oriented or every loop has been oriented. Observe that, as every portion of loop sees the loop that overflies it, this process terminates.

Definition 2. *A* well-labeled unicellular mobile *is a labeled unicellular mobile that satisfies the properties of Lemma 3.(ii) and such that the previous process only creates well oriented level loops.*

We now suppose that $(\mathfrak{u}, \mathfrak{l})$ is a well-labeled unicellular mobile and we perform the previous construction. We denote by $\mathfrak{m}$ the map whose vertex set is $V_\circ(\mathfrak{u}) \cup \{v^\bullet\}$, whose edges are the black edges and whose root is the future root. We also denote by $\bar{\mathfrak{m}}$ the root flipped version of $\mathfrak{m}$ and set $\Psi((\mathfrak{u}, \mathfrak{l}), +) := (\mathfrak{m}, v^\bullet)$ and $\Psi((\mathfrak{u}, \mathfrak{l}), -) := (\bar{\mathfrak{m}}, v^\bullet)$. See Figure 14 and Figure 24.

3.2.3 A note on the orientable case

If $\mathcal{S}$ is orientable, we recover the condition of [BDG04]: a labeled unicellular mobile $(\mathfrak{u}, \mathfrak{l})$ is well labeled if and only if $\mathfrak{l}(c') \geq \mathfrak{l}(c) - 1$ whenever the corner c' directly follows the corner c in the contour order of the face of $\mathfrak{u}$, oriented in the orientation induced by the root of $\mathfrak{u}$. Indeed, in this case, the whole surface is oriented in the orientation prescribed by the root and all the loops are oriented in the opposite orientation around $v^\bullet$. Then the conjunction of the fact that all the loops are well oriented with Lemma 3.(ii)(c) becomes the following condition. For all $i \geq 2$ and for every corner with label i, the first subsequent corner with label strictly smaller than i has label $i-1$. This is clearly equivalent to the claimed condition.

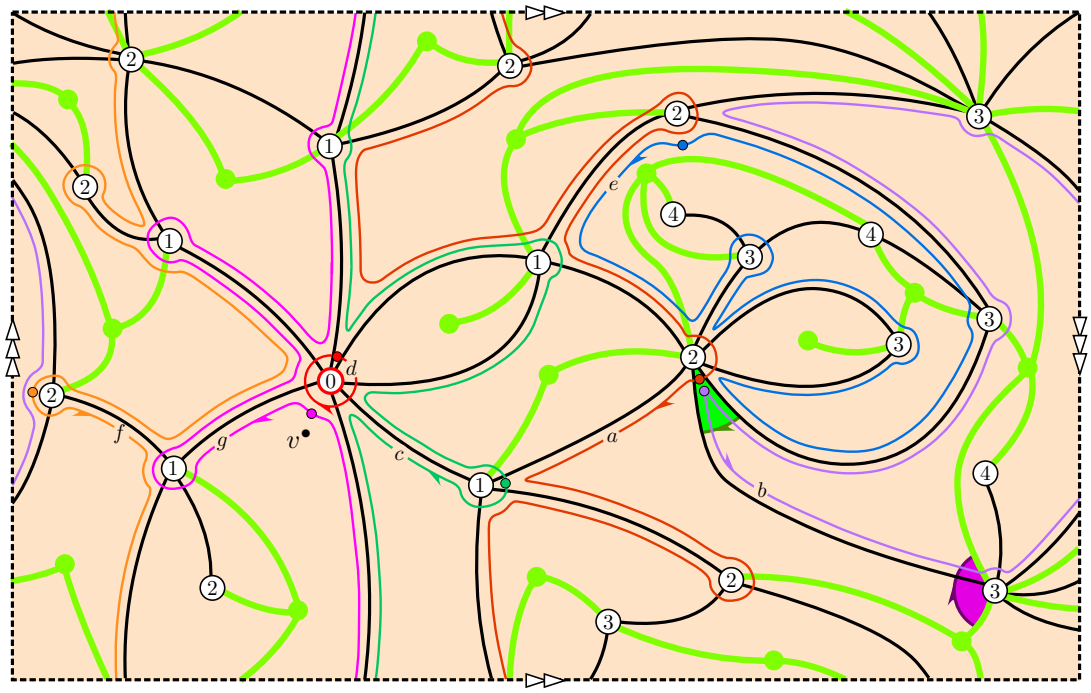

Figure 14: *The bijection, from a well-labeled unicellular mobile to a pointed bipartite map.*

3.3 The previous mappings are inverse one from another

We denote by $\mathcal{B}^\bullet$ the set of pointed bipartite maps of the surface $\mathcal{S}$ we consider and by $\mathcal{U}$ the set of well-labeled unicellular mobiles (defined in Section 3.2). Recall that we denoted by Φ the mapping from Section 3.1 and by Ψ the one from Section 3.2.

Proposition 4. *Let* $(\mathfrak{m}, v^\bullet) \in \mathcal{B}^\bullet$ *and* $((\mathfrak{u}, \mathfrak{l}), \varepsilon) := \Phi(\mathfrak{m}, v^\bullet)$. *Then*

(i) $V(\mathfrak{m}) = V_\circ(\mathfrak{u}) \sqcup \{v^\bullet\}$ *and, for* $v \in V_\circ(\mathfrak{u})$, $\mathfrak{l}(v) = d_\mathfrak{m}(v, v^\bullet)$;

(ii) the faces of $\mathfrak{m}$ *correspond to* $V_\bullet(\mathfrak{u})$*: moreover, the degree of a face of* $\mathfrak{m}$ *is twice the degree of the corresponding vertex in* $V_\bullet(\mathfrak{u})$;

(iii) the maps $\mathfrak{m}$ *and* $\mathfrak{u}$ *have the same number of edges.*

Proof. Statement (*i*) and the fact that the faces of $\mathfrak{m}$ correspond to the green vertices of $\mathfrak{u}$ are direct consequences of the construction. Let us consider a face of $\mathfrak{m}$ and denote by $2p$ its degree. We see the face as a $2p$-gon and pair its sides as follows. Let us pick a side and denote by i and $i+1$ the labels of its extremities. We travel along the boundary from the vertex labeled $i+1$ to the vertex labeled i and we keep traveling until we successively encounter a corner labeled i and a corner labeled $i+1$. We match the side we picked with the side linking these corners (note that these two sides are necessarily distinct and that the matching does not depend on which of the two sides we first picked). This gives a perfect matching of the sides of our polygon.

We then consider a loop at level $i+1$ that visits the face. Recall that this loop selects the corners with label $i+1$ that are immediately preceded by a corner labeled i. Then by construction of the loop, if a corner labeled $i+1$ of our face is selected, then the previous corner labeled i that the loop visits also belongs to our face; we associate with the selected corner the side linking these two corners. Now observe that two paired sides with labels i - $i+1$ are visited by the same portion of level loop at level $i+1$, one from label $i+1$ to label i and the other one from label i to label $i+1$. As a result, exactly one of these two sides is associated with a selected corner. As there are p pairs of sides, there are also p selected corners and the green vertex of the face has degree p.

Point *(iii)* is then a direct consequence of *(ii)*: the number of edges of $\mathfrak{m}$ is half the sum of the degrees of its faces and the number of edges of $\mathfrak{u}$ is equal to the sum of the degrees of its green vertices. □

Theorem 5. *The mappings $\Phi : \mathcal{B}^\bullet \to \mathcal{U} \times \{+,-\}$ and $\Psi : \mathcal{U} \times \{+,-\} \to \mathcal{B}^\bullet$ are bijections, which are inverse one from another.*

Using Proposition 4, we obtain the following specialization of Theorem 5. For an integer finite sequence $\alpha = (\alpha_1, \ldots, \alpha_n)$, we denote by $\mathcal{B}^\bullet_\alpha$ the set of bipartite maps of $\mathcal{S}$ with n faces marked 1, 2, …, n and such that, for $1 \le i \le n$, the face marked i has degree $2\alpha_i$. We also denote by $\mathcal{U}_\alpha$ the set of well-labeled unicellular mobiles with n green vertices marked 1, 2, …, n and such that, for $1 \le i \le n$, the green vertex marked i has degree α_i.

Corollary 6. *The restriction of Φ to $\mathcal{B}^\bullet_\alpha$ realizes a bijection between $\mathcal{B}^\bullet_\alpha$ and $\mathcal{U}_\alpha \times \{+,-\}$.*

We may now come back to the case of quadrangulations.

Corollary 7. *The mappings of Section 2 are inverse bijections.*

Proof. By Proposition 4.*(ii)* and Theorem 5, the restrictions of Φ and Ψ are bijections between bipartite quadrangulations and pairs of a well-labeled unicellular mobile with green vertices of degree 2 and a parameter in $\{+,-\}$.

From a well-labeled unicellular mobile with green vertices of degree 2, we can remove the green vertices and merge the two incident edges into single edges. Let us consider two neighboring vertices in the resulting map with labels i and j with $i > j$. Then a level loop at level $i-1$ passes through the edge so that it can only be well oriented if $j = i-1$. We obtain that the resulting map is a well-labeled unicellular map, as defined in Section 2.

Reciprocally, starting from a well-labeled unicellular map and adding a green vertex on every edges gives a labeled unicellular mobile satisfying the properties of Lemma 3.*(ii)*. Clearly, every nontrivial arc of such a mobile has the same label at both extremities, so that every orientation of any loop is always a good orientation. As a result, we obtain a well-labeled unicellular mobile with green vertices of degree 2.

The mappings presented in Section 2 are respectively the composition of Φ with the removal of green vertices and the composition of the addition of green vertices on the edges with Ψ. □

Proof of Theorem 5. It is sufficient to show that

(*a*) If $(\mathfrak{u}, \mathfrak{l}) \in \mathcal{U}$, $\varepsilon \in \{+,-\}$ and $(\mathfrak{m}, v^\bullet) = \Psi((\mathfrak{u}, \mathfrak{l}), \varepsilon)$, then $(\mathfrak{m}, v^\bullet) \in \mathcal{B}^\bullet$ and $\Phi(\mathfrak{m}, v^\bullet) = ((\mathfrak{u}, \mathfrak{l}), \varepsilon)$.

(*b*) If $(\mathfrak{m}, v^\bullet) \in \mathcal{B}^\bullet$ and $((\mathfrak{u}, \mathfrak{l}), \varepsilon) = \Phi(\mathfrak{m}, v^\bullet)$, then $(\mathfrak{u}, \mathfrak{l}) \in \mathcal{U}$ and $\Psi((\mathfrak{u}, \mathfrak{l}), \varepsilon) = (\mathfrak{m}, v^\bullet)$.

Let us show (*a*). Let $(\mathfrak{u}, \mathfrak{l}) \in \mathcal{U}$ and denote by $(\mathfrak{m}, v^\bullet) \coloneqq \Psi((\mathfrak{u}, \mathfrak{l}), +)$. It will be enough to show that $(\mathfrak{m}, v^\bullet) \in \mathcal{B}^\bullet$ and $\Phi(\mathfrak{m}, v^\bullet) = ((\mathfrak{u}, \mathfrak{l}), +)$, as this immediately implies that $(\bar{\mathfrak{m}}, v^\bullet) = \Psi((\mathfrak{u}, \mathfrak{l}), -) \in \mathcal{B}^\bullet$ and $\Phi(\bar{\mathfrak{m}}, v^\bullet) = ((\mathfrak{u}, \mathfrak{l}), -)$.

Recall that every corner of $\mathfrak{u}$ corresponds to a black edge. If a corner c has label i, then the black edge links it to a corner with label $i-1$. Let us call this corner the *successor* of c. By construction, if $i \geq 2$, this corner is one of the two corners appearing in the statement of Lemma 3.(*ii*)(*c*). Moreover, if we consider an $\{i, j\}$-arc with $i \geq j$, then either the $(i-j)$-th successor of the extremity labeled i is the extremity labeled j or the $(i-j+1)$-th successor of the extremity labeled i is the successor of the extremity labeled j (if $i = j$, we are necessarily in the second case). In particular, the extremities of an arc are always linked by a chain of black edges.

We now consider a connected component of the complement of $\mathfrak{m}$. It consists of a finite union of connected components delimited by two green edges incident to the same green vertex corresponding to some trivial arc and by the chain of black edges linking the extremities of this trivial arc. These components are glued together at the green edges incident to the same green vertex and we see that the considered connected component is homeomorphic to a disk and contains only one green vertex. As a result, $\mathfrak{m}$ is a map and it is bipartite as every black edge links a vertex with odd label to a vertex with even label.

As $(\mathfrak{m}, v^\bullet) \in \mathcal{B}^\bullet$, we can apply to it the construction of Section 3.1. First, notice that the labels of $V(\mathfrak{m})$ are given by $\mathfrak{l}$. Indeed, $\mathfrak{l}(v^\bullet) = 0$ and if $v \neq v^\bullet$, then, as the variation of $\mathfrak{l}$ along any black edge is 1, every black path from $v^\bullet$ to v has length at least $\mathfrak{l}(v)$. Moreover, taking a corner incident to v and following the black edges linking it to its subsequent successors provides a path from v to $v^\bullet$ of length $\mathfrak{l}(v)$. In particular, we furthermore immediately obtain that the root vertex of $\mathfrak{m}$ has a smaller label than the other extremity of the root edge of $\mathfrak{m}$ (see Figure 8), which entails that the second coordinate of $\Phi(\mathfrak{m}, v^\bullet)$ will be set to $+$.

Let us consider an unoriented level loop at level i of $(\mathfrak{u}, \mathfrak{l})$ and one of the arcs it delimits. By construction, the level loop follows the chain of black edges linking the extremities of the arc and, if the arc has level i, at one of its extremities, the level loop crosses the black edges linking the corners of the arc with label $i+1$. (If the arc has level strictly smaller than i, it is necessarily trivial.) As the labels along the chain of black edges are all smaller than i, we see that the unoriented level loop is exactly an unoriented level loop of $(\mathfrak{m}, v^\bullet)$. As every side of every black edge starting from a corner labeled i is visited by exactly one level loop of $(\mathfrak{u}, \mathfrak{l})$ and one level loop of $(\mathfrak{m}, v^\bullet)$, we conclude that the unoriented level loops are exactly the same for both constructions. And as the orientation process for the loops is clearly the same for both constructions, we see that the level loops coincide.

Let us now consider a level loop at level i and see which corners of $\mathfrak{m}$ it selects. We consider an arc it delimits. If the level of this arc is strictly smaller than i, the loop does not select any corners. If the arc has level i, then the loop first visits half a corner of $\mathfrak{m}$ (the corner delimited by a green edge and a black edge), then a certain number of corners of $\mathfrak{m}$ labeled i before traveling along the chain of black edges linking the extremities of the arc and finally, the loop visits the other extremity of the arc, which also corresponds to half a corner of $\mathfrak{m}$ (see Figure 13). All the corners of $\mathfrak{m}$ visited along the chain of black edges have labels strictly smaller than i so that the only corners of $\mathfrak{m}$ that this portion of loop can select are the half-corners. Moreover, the second half-corner is selected if and only if its label is equal to i. It is in this case indeed preceded by a corner of $\mathfrak{m}$ labeled $i-1$. As every first half-corner in an arc is matched with a second half-corner in some arc (the same one or another one), we conclude that the selected corners of $\mathfrak{m}$ are exactly those from where a green edge starts. As every face of $\mathfrak{m}$ contains exactly one green vertex, the later must be connected to

the selected corners by green edges. As the rooting convention for $\Phi(\mathfrak{m}, v^\bullet)$ clearly gives the root of $(\mathfrak{u}, \mathfrak{l})$, we conclude that $\Phi(\mathfrak{m}, v^\bullet) = ((\mathfrak{u}, \mathfrak{l}), +)$, as desired.

We now turn to (*b*)**.** Let $(\mathfrak{m}, v^\bullet) \in \mathcal{B}^\bullet$ and $((\mathfrak{u}, \mathfrak{l}), \varepsilon) = \Phi(\mathfrak{m}, v^\bullet)$. Adapting arguments from [CMS09], we start by showing that the embedded graph $\mathfrak{u}$ is a unicellular map. We consider the map $\mathfrak{M}$ whose vertex set is $V(\mathfrak{m}) \cup V_\bullet(\mathfrak{u})$ and whose edges are the edges of $\mathfrak{m}$ together with the edges of $\mathfrak{u}$. We add inside each face of this map a blue vertex and, for each edge of $\mathfrak{m}$, we add a blue dual edge linking the blue vertices of the two incident faces[2]. Let us see that this embedded blue graph has only one cycle, which turns around $v^\bullet$. To this end, let us label each blue edge by the minimal label of the extremities of the black edge it crosses. Let us consider a blue cycle and denote by m the maximal label of its edges. Let us consider a blue edge e of the cycle with label m and a neighboring edge e' of the cycle. See Figure 15.

Let $\tilde{e}$ and $\tilde{e}'$ denote the black dual edges of e and e'. These edges are incident to the same face of $\mathfrak{m}$, which is split into two connected components by $e \cup e'$; we denote by v the extremity of $\tilde{e}$ labeled m and by v' the extremity of $\tilde{e}'$ incident to the same connected component as v. As all the corners whose label is a local maximum are selected by the level loops, the green vertex must belong to the connected component that does not contain v (recall that $\ell(v') \leq m$). As a result, all the vertices of the connected component containing v are not selected and are thus not local maximums. In particular, if $v' \neq v$, as $\ell(v') \leq m$, the neighboring vertex of v must be labeled $m-1$. We conduct the same reasoning with the blue edge e'' of the cycle that intersects the other extremity of e and denote by $\tilde{e}''$ and v'' the counterparts of $\tilde{e}'$ and v'. We see that, if v, v' and v'' are three pairwise distinct vertices, there must exist a level loop at level m that crosses $\tilde{e}$. This loop should select a corner labeled $m-1$, which is impossible. As a result, either $v' = v$ or $v'' = v$.

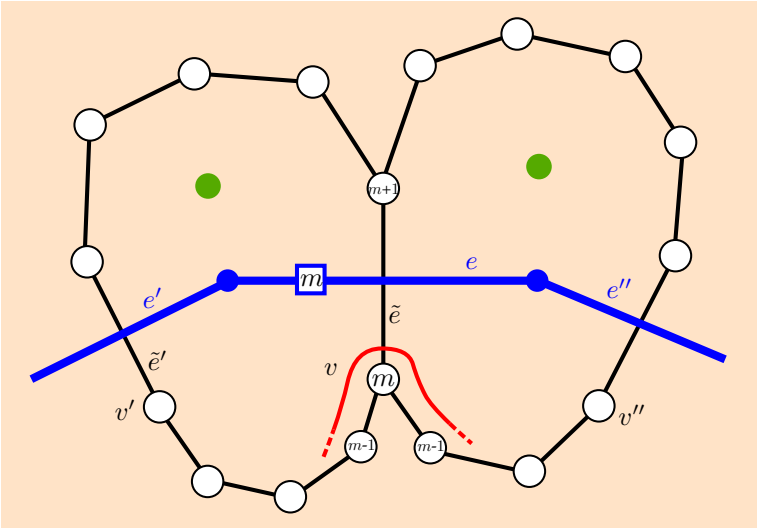

Figure 15: *Proof that* $\mathfrak{u}$ *is a unicellular map. The part of level loop is represented in red.*

[2]The embedded blue graph we obtain is a generalization of the *dual exploration graph* appearing in [CD15] (and also represented in blue on the Figures of this reference).

Without loss of generality, let us suppose that $v' = v$. Let us furthermore suppose for now that the other extremity of $\tilde{e}'$ has label $m-1$. In this case, the level loop is still present and we must have $v'' = v$. If the other extremity of $\tilde{e}''$ also has label $m-1$, the level loop is still present and we obtain a contradiction. We must thus have that the other extremity of $\tilde{e}''$ also has label $m+1$ and as a consequence, e'' has label m. We iterate the argument with the blue edges succeeding e'' in the cycle and obtain that every edge of the cycle has label m, a contradiction with our hypothesis that e' had label $m-1$. In the end, we obtain that e' has label m and, iterating the argument, we finally obtain that the blue cycle turns around a single vertex that is a local minimum for the labels. This vertex is thus necessarily $v^\bullet$.

We can then retract to 0 each connected component of the complement of $\mathfrak{u}$ along the corresponding connected component of the blue graph. As a result, we obtain that $\mathfrak{u}$ is a map and we conclude that it is unicellular by Euler's characteristic formula, noting that it has $v(\mathfrak{m}) - 1 + f(\mathfrak{m})$ vertices and $e(\mathfrak{m})$ edges by Proposition 4, where we denoted by $v(\mathfrak{m})$, $f(\mathfrak{m})$ and $e(\mathfrak{m})$ the number of vertices, faces and edges of $\mathfrak{m}$.

We obtained that $(\mathfrak{u}, \mathfrak{l})$ was a labeled unicellular mobile. Let us now show that it satisfies the properties of Lemma 3.(*ii*). We consider a corner of $\mathfrak{u}$ with label i. We first claim that there is a black edge linking it to a vertex labeled $i-1$. Indeed, consider all the black edges starting from this corner. The selection process of corners by level loops ensures that there is at least one such edge. If all these edges were linking the corner to vertices labeled $i+1$, the level loop at level i would cross all these edges while turning around the vertex incident to the corner and, as a result, at most one of the two green edges incident to the corner would exist. This is a contradiction. Moreover, by Proposition 4, there are exactly as many black edges as corners of $\mathfrak{u}$ so that there is actually exactly one black edge per corner labeled i linking it to a vertex labeled $i-1$ and every black edge is of this form.

We furthermore suppose that $i \geq 2$ and we let e be the black edge corresponding to our considered corner. As both extremities of e belong to $V(\mathfrak{u})$ and $\mathfrak{u}$ is unicellular, e splits the face of $\mathfrak{u}$ into two connected components: let us focus on the one that does not contain $v^\bullet$. The boundary of this component consists of a chain of green edges together with e. Let c be a corner on the chain with minimal label. We claim that c is necessarily the corner where e ends. Indeed, the black edge corresponding to c links it to a vertex with strictly smaller label, which by definition does not belong to the chain. As this edge cannot cross e, c must be an extremity of the chain. From this, we obtain that $(\mathfrak{u}, \mathfrak{l})$ satisfies Lemma 3.(*ii*)(*c*).

We may then proceed with the construction of Section 3.2. Let us consider a level loop of $\mathfrak{m}$ at level $i \geq 1$. As it selects at least one corner, it has to cross a green edge. We consider a portion of this level loop completely included in the face of $\mathfrak{u}$ and the chain of green edges it delimits. We claim this chain corresponds to an arc. Indeed, the portion of loop travels along a chain of black edges linking the extremities of the green chain, crossing possibly only edges of type i-$i+1$. This black chain splits the face of $\mathfrak{u}$ into two connected components, and $v^\bullet$ is either on the black chain or in the component not containing the portion of loop, as the latter only crosses edges of type i-$i+1$. Then a corner with minimal label on the green chain must be linked by a chain of black edges to $v^\bullet$, going through decreasing labels and this chain cannot intersect the black chain along which the portion of loop travels. This is only possible if the corner is an extremity of the green chain and this implies that the green chain corresponds to an arc as claimed. Moreover, if it is nontrivial, its level is i.

From this, we deduce that the unoriented level loops of $\mathfrak{m}$ coincide with the unoriented level loops of $\mathfrak{u}$. Let us consider a portion of level loop at level i delimiting some nontrivial arc at

level i. We orient this portion of loop by the orientation process of $\mathfrak{m}$. The portion of loop enters the face of $\mathfrak{u}$ by an extremity of the arc and exits by the other extremity. It only crosses edges of type i-$i+1$ at the extremity by which it enters, as otherwise, it would have selected the last corner of $\mathfrak{m}$ it visits before crossing an edge of type i-$i+1$ at the extremity by which it exits. As a result, the orientation of the loops induced by $\mathfrak{m}$ give the right identifications of temporary vertices. Comparing the orientation processes as well as the rooting processes, we conclude that $(\mathfrak{u}, \mathfrak{l})$ is a well-labeled unicellular map and that $\Psi((\mathfrak{u}, \mathfrak{l}), \varepsilon) = (\mathfrak{m}, v^\bullet)$, as desired. □

4 General maps

4.1 The mappings

We now relax the hypothesis that the map is bipartite. We will slightly modify it in order to be able to apply our bijection from Section 3.1. We denote by $\mathcal{M}^\bullet$ the set of pointed maps of $\mathcal{S}$ and by $\mathcal{M}^\bullet_{\mathrm{eq}}$ its subset consisting of pointed maps such that both extremities of the root edge are at same distance from the distinguished vertex.

We consider a general pointed map $(\mathfrak{m}, v^\bullet) \in \mathcal{M}^\bullet$ and define the labeling function $\mathfrak{l} : V(\mathfrak{m}) \to \mathbb{Z}_+$ as before. There are now two kinds of edges: an edge will be called *equilabeled* if its extremities both have the same label. We then enlarge the map $\mathfrak{m}$ by adding in the middle of each equilabeled edge an extra vertex splitting the edge into two new edges. We denote by $\tilde{\mathfrak{m}}$ this enlarged map and we assign to each added vertex the common label of its two neighbors plus 1. This extends the definition of $\mathfrak{l}$ to $V(\tilde{\mathfrak{m}})$ and, clearly, for $v \in V(\tilde{\mathfrak{m}})$, one has $\mathfrak{l}(v) = d_{\tilde{\mathfrak{m}}}(v^\bullet, v)$. See Figure 16.

The map $\tilde{\mathfrak{m}}$ is bipartite, so we may apply the construction of Section 3.1: we set $((\tilde{\mathfrak{u}}, \mathfrak{l}), \varepsilon) := \Phi(\tilde{\mathfrak{m}}, v^\bullet)$. Note that we necessarily have $\varepsilon = +$ in the case $(\mathfrak{m}, v^\bullet) \in \mathcal{M}^\bullet_{\mathrm{eq}}$. We slightly modify the encoding map as follows. Every vertex of $V(\tilde{\mathfrak{m}}) \setminus V(\mathfrak{m})$ is by design of degree 2 and both corners incident to it are selected by the level loops, as they correspond to local maximums along the boundaries of the incident faces. As a result, it also has degree 2 in $\tilde{\mathfrak{u}}$; we suppress it and merge the two incident edges into a single edge. We call such a resulting edge a *flagged edge* and we assign to it the label of the suppressed vertex. We denote by $(\mathfrak{u}, \mathfrak{l})$ the resulting map, the function $\mathfrak{l}$ being defined on a subset of the vertices and edges of $\mathfrak{u}$. Finally, if the root edge of $\mathfrak{m}$ is equilabeled, then the root vertex of $\tilde{\mathfrak{u}}$ is one of the added vertices of $\tilde{\mathfrak{m}}$. In this case, we transgress our usual definition of root and declare the root of $\mathfrak{u}$ to be the edge resulting of the suppression of the root vertex of $\tilde{\mathfrak{u}}$, together with the side and local orientation induced by the root of $\tilde{\mathfrak{u}}$. Such a map will be called *edge-rooted* in what follows. See Figure 17.

We extend the definition of Φ by setting $\Phi(\mathfrak{m}, v^\bullet) := ((\mathfrak{u}, \mathfrak{l}), \varepsilon)$. Plainly, if $\mathfrak{m}$ is bipartite, then $\tilde{\mathfrak{m}} = \mathfrak{m}$ and $((\tilde{\mathfrak{u}}, \mathfrak{l}), \varepsilon) = ((\mathfrak{u}, \mathfrak{l}), \varepsilon)$ so that the definition of Φ is consistent with the previous definition from Section 3.1. A *labeled generalized unicellular mobile* is a pair $(\mathfrak{u}, \mathfrak{l})$ such that

- $\mathfrak{u}$ is a rooted or edge-rooted one-face map of $\mathcal{S}$ whose vertex set is partitioned into $V_\bullet(\mathfrak{u}) \sqcup V_\circ(\mathfrak{u})$ in such a way that every edge has at least one extremity in $V_\bullet(\mathfrak{u})$;
- if $\mathfrak{u}$ is rooted, its root vertex lies in $V_\circ(\mathfrak{u})$; if $\mathfrak{u}$ is edge-rooted, its root edge belongs to the set $E_\diamond(\mathfrak{u})$ of edges linking two vertices of $V_\bullet(\mathfrak{u})$;
- $\mathfrak{l} : V_\circ(\mathfrak{u}) \sqcup E_\diamond(\mathfrak{u}) \to \mathbb{N}$ is a function with minimum 1.

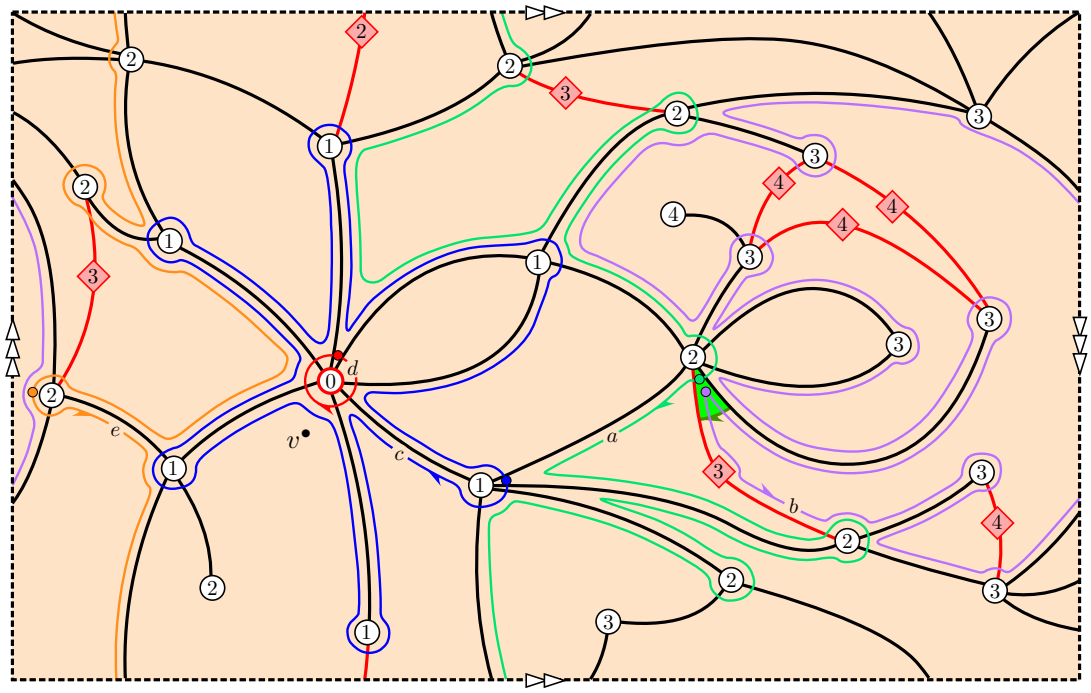

Figure 16: *The level loops for a general map. The equilabeled edges are represented in red and the added vertices are represented by red squares. As above, the maximal level loops are not represented.*

The edges of $E_\diamond(\mathfrak{u})$ are called *flagged edges*. We define the following *flag splitting operation* on the set of labeled generalized unicellular mobiles. Given a labeled generalized unicellular mobile, we split each flagged edge into two edges by adding a vertex in the middle and we assign to the added vertex the label of the flagged edge. If the original map is edge-rooted, we root the resulting map at the corner incident to the vertex added on the root edge that corresponds to the distinguished side of the root edge, oriented in accordance with the root orientation of the original map. We obtain by this operation a labeled unicellular mobile.

A labeled generalized unicellular mobile is called a *well-labeled generalized unicellular mobile* if the flag splitting operation makes it a well-labeled unicellular mobile and if, in the construction of Section 3.2 applied to the resulting well-labeled unicellular mobile, the temporary vertices are never identified with vertices added during the flag splitting operation.

Let $(\mathfrak{u}, \mathfrak{l})$ be a well-labeled generalized unicellular mobile, let $(\tilde{\mathfrak{u}}, \mathfrak{l})$ denote the well-labeled unicellular mobile obtained by the flag splitting operation and let $(\tilde{\mathfrak{m}}, v^\bullet) := \Psi((\tilde{\mathfrak{u}}, \mathfrak{l}), +)$. Let $v \in V(\tilde{\mathfrak{u}}) \setminus V(\mathfrak{u})$. It has degree 2 in $\tilde{\mathfrak{u}}$ so it has degree at least 2 in $\tilde{\mathfrak{m}}$. But the condition that the temporary vertices in the construction of Section 3.2 are not identified with v ensures that v has degree exactly 2 in $\tilde{\mathfrak{m}}$. As a result, we may define the map $\mathfrak{m}$ by suppressing from $\tilde{\mathfrak{m}}$ each vertex of $V(\tilde{\mathfrak{u}}) \setminus V(\mathfrak{u})$ and by merging the two incident edges into a single edge. Note that neither $v^\bullet$ nor the root vertex of $\tilde{\mathfrak{m}}$ are suppressed, so that the pointed map $(\mathfrak{m}, v^\bullet)$ is well defined.

We extend the definition of Ψ by setting $\Psi((\mathfrak{u}, \mathfrak{l}), +) := (\mathfrak{m}, v^\bullet)$ and, whenever $(\mathfrak{u}, \mathfrak{l})$ is not edge-rooted, $\Psi((\mathfrak{u}, \mathfrak{l}), -) := (\tilde{\mathfrak{m}}, v^\bullet)$. We denote by $\mathcal{G}$ the set of well-labeled generalized unicellular

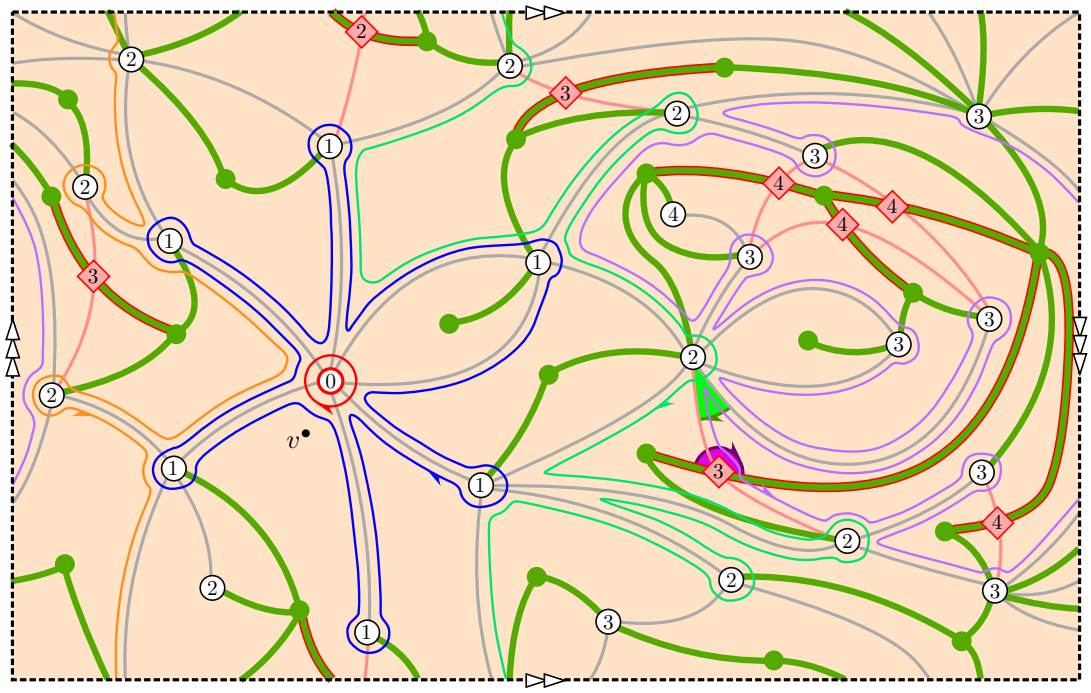

Figure 17: *The bijection for a general map. The flagged edges of the mobile have been highlighted and their labels are represented by the red squares. On this example, the root edge is equilabeled; the root of the mobile is thus a flagged edge given with a side and local orientation.*

mobiles and by $\mathcal{G}_{\mathrm{er}} \subset \mathcal{G}$ the subset of edge-rooted ones. If $(\mathfrak{u}, \mathfrak{l}) \in \mathcal{G}$, the *generalized degree* of a vertex in $V_\bullet(\mathfrak{u})$ is defined as the number of incident nonflagged edges plus half the number of incident flagged edges (counted with multiplicity). We readily obtain the following theorem.

Theorem 8. *The extended mappings Φ and Ψ induce bijections between $\mathcal{M}^\bullet_{\mathrm{eq}}$ and $\mathcal{G}_{\mathrm{er}} \times \{+\}$ on the one hand, and between $\mathcal{M}^\bullet \setminus \mathcal{M}^\bullet_{\mathrm{eq}}$ and $\mathcal{G} \setminus \mathcal{G}_{\mathrm{er}} \times \{+,-\}$ on the other hand, and these bijections are inverse one from another.*

Moreover, if $(\mathfrak{m}, v^\bullet) \in \mathcal{M}^\bullet$ and $((\mathfrak{u}, \mathfrak{l}), \varepsilon) = \Phi(\mathfrak{m}, v^\bullet)$, then

(i) $V(\mathfrak{m}) = V_\circ(\mathfrak{u}) \sqcup \{v^\bullet\}$ *and, for* $v \in V_\circ(\mathfrak{u})$, $\mathfrak{l}(v) = d_{\mathfrak{m}}(v, v^\bullet)$;

(ii) the faces of $\mathfrak{m}$ correspond to $V_\bullet(\mathfrak{u})$: moreover, the degree of a face of $\mathfrak{m}$ is twice the generalized degree of the corresponding vertex in $V_\bullet(\mathfrak{u})$;

(iii) the maps $\mathfrak{m}$ and $\mathfrak{u}$ have the same number of edges.

We may specialize this theorem by prescribing the face degrees as we did in Corollary 6. For a finite integer sequence $\alpha = (\alpha_1, \dots, \alpha_n)$, we denote by $\mathcal{M}^\bullet_\alpha$ the set of maps of $\mathcal{S}$ with n faces marked $1, 2, \dots, n$ and such that, for $1 \le i \le n$, the face marked i has degree α_i. We also denote by $\mathcal{G}_\alpha$ the set of well-labeled generalized unicellular mobiles with n green vertices marked $1, 2, \dots, n$ and such that, for $1 \le i \le n$, the green vertex marked i has generalized degree $\alpha_i/2$.

Corollary 9. *The restriction of Φ to $\mathcal{M}^\bullet_\alpha$ realizes a bijection between $\mathcal{M}^\bullet_\alpha$ and $(\mathcal{G}_\alpha \times \{+,-\}) \setminus (\mathcal{G}_{\mathrm{er}} \times \{-\})$.*

4.2 Application to triangulations

The bijection

We saw in Section 2 that the bijections were more convenient for quadrangulations. In particular, the labels on the encoding objects only satisfied *local* constraints instead of global ones as it is the case in general. As noted during the proof of Corollary 7, every orientation of a level loop is always good, so that the global constraints are automatically satisfied. In the case of triangulations, the same argument holds and we can thus give a simpler characterization of the encoding objects and derive enumeration results.

Let us look at the restriction of Φ to the set $\mathcal{T}^\bullet$ of pointed triangulations. By Theorem 8, every green vertex of a corresponding element of $\mathcal{G}$ is either exactly incident to 3 flagged edges or exactly incident to one nonflagged edge and one flagged edge. Moreover, the labels around a green vertex can only be of the three types depicted on Figure 18.

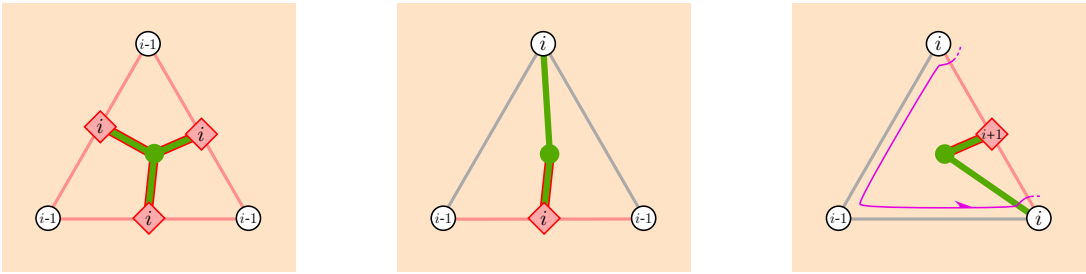

Figure 18: *The three possible types of face and the corresponding green vertices.*

Let us denote by $\mathcal{E}$ the set of labeled generalized unicellular mobile with green vertices of generalized degree $3/2$ and such that the labels around any green vertex are of a type shown on Figure 18. Plainly, the label variations along two consecutive corners of an element of $\mathcal{E}$ belong to $\{-1, 0, 1\}$. As in the case of quadrangulations, this entails that such an element satisfies the properties of Lemma 3.(*ii*), that every of its nontrivial arcs has the same label at both extremities, and finally that every orientation of any of its level loops is a good orientation. Moreover, the conditions on the labels entail that both extremities of every nontrivial arc are original white vertices (in the sense that they were not added during the flag splitting operation) so that no temporary vertices will be identified with vertices added during the flag splitting operation. Denoting by $\mathcal{E}_{\mathrm{er}}$ the set of edge-rooted mobiles from $\mathcal{E}$, we obtain the following corollary.

Corollary 10. *The restriction of Φ to $\mathcal{T}^\bullet$ realizes a bijection between $\mathcal{T}^\bullet$ and $(\mathcal{E} \times \{+, -\}) \setminus (\mathcal{E}_{\mathrm{er}} \times \{-\})$. Moreover, the corresponding objects have the same number of edges.*

Generating functions

From now on, it will be convenient to slightly modify the bijection of Corollary 10 by subtracting $1/2$ from all the labels of the flagged edges. This will bring some symmetry and make the computation easier. Note that this also makes sense from a metric point of view, as the labels now represent the distances to the distinguished vertex in the metric space obtained from the triangulation by replacing each edge by a unit length segment. We furthermore consider from now on

labeled generalized unicellular mobiles up to addition of an integer constant to all the labels. We will decompose these mobiles into elementary pieces in order to count them. We use the framework of [CMS09, CD15].

We first consider nonrooted plane labeled generalized unicellular mobiles with one green vertex incident to exactly one edge and such that every other green vertex is incident to exactly

- ◇ either 3 flagged edges with the same label
- ◇ or one flagged edge with some label $i \in \mathbb{Z} + \frac{1}{2}$ and one nonflagged edge incident to a white vertex with label $i \pm \frac{1}{2}$.

We introduce the generating function F (resp. N) counting with weight t per edge (flagged or nonflagged) such objects with the extra condition that the isolated green vertex is incident to a flagged (resp. nonflagged) edge. The decomposition depicted on Figure 19 yields

$$F = tF^2 + 2tN \qquad \text{and} \qquad N = t + 2tNF. \tag{1}$$

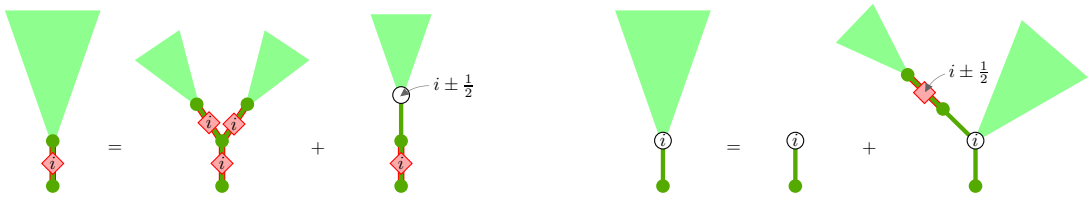

Figure 19: *Elementary decomposition of F-mobiles and N-mobiles.*

Let us call *F-mobile* and *N-mobile* the objects counted by F and N. When we fix a representative of the labels of an F-mobile (resp. an N-mobile), we call label of the mobile the label of the flagged edge (resp. of the white vertex incident to the nonflagged edge) that is incident to the isolated green vertex.

For i, $j \in \mathbb{Z}$, we introduce the generating function $C_{i,j}$ of nonrooted plane generalized unicellular mobiles whose green vertices satisfy the previous itemized conditions, with two **distinct** distinguished white vertices labeled i and j. We extend the definition to $i \in \mathbb{Z} + \frac{1}{2}$ by replacing the distinguished white vertex labeled i by a green vertex incident to exactly one flagged edge labeled i. Similarly, we extend the definition to every $i, j \in \mathbb{Z}/2$.

In order to compute $C_{i,j}$, we start by considering the following objects. We link the isolated green vertices of two N-mobiles by a chain of flagged edges and we graft an F-mobile onto every green vertex of the chain that is incident to two flagged edges. Every F-mobile can be grafted either on one side or on the other side of the chain. We furthermore impose that the labels of the resulting plane mobile satisfy the previous conditions. If we let i and j be the labels of the N-mobiles, the only possibilities are $j \in \{i-1, i, i+1\}$. Moreover, all the flagged edges of the chain and all the grafted F-mobiles must have the same label, which is $i+1/2$ if $j = i+1$, $i-1/2$ if $j = i-1$, or $i \pm 1/2$ if $j = i$. As a result, the generating function of these objects is $tN^2/(1-2tF) = N^3$ if $j = i \pm 1$ and $2N^3$ if $j = i$.

We then consider Motzkin words, that is, finite sequences of -1, 0 or $+1$. We count them with a weight $Z := N^3$ per ± 1 and $2Z$ per 0. Let us call *increment* of a Motzkin word $w_1 w_2 \dots w_n$ the

integer $\sum_{k=1}^{n} w_k$. We denote by U the generating function of words $w_1 w_2 \dots w_n$ with increment -1 and such that $\sum_{k=1}^{l} w_k \geq 0$ for $1 \leq l < n$, and by B the generating function of words with increment 0. Considering whether the first letter is -1, 0 or $+1$, we obtain

$$U = Z + 2Z\,U + Z\,U^2 \qquad \text{and} \qquad B = 1 + Z\,UB + 2Z\,B + Z\,UB$$

so that

$$Z = \frac{U}{(1+U)^2}\,, \qquad B = \frac{1+U}{1-U}\,, \qquad U = \frac{1-\sqrt{1-4Z}}{2Z} - 1. \tag{2}$$

The generating function of Motzkin words with increment $\ell \in \mathbb{Z}$ is then equal to $BU^{|\ell|}$.

We may now explicit $C_{i,j}$. Let us first suppose that $i, j \in \mathbb{Z}$. The differences between the labels of subsequent white vertices on the path linking the two distinguished vertices form a nonempty Motzkin word. Decomposition at these vertices yields $C_{i,j} = BU^{|j-i|} - \mathbb{1}_{\{i=j\}}$. Now, if $i \in \mathbb{Z} + \frac{1}{2}$, $j \in \mathbb{Z}$, we have $C_{i,j} = N^2(BU^{|j-i-\frac{1}{2}|} + BU^{|j-i+\frac{1}{2}|}) = B\sqrt{N}U^{|j-i|}$. Similar computations show that, for $i, j \in \mathbb{Z}/2$, we have

$$C_{i,j} = BN^{\frac{1}{2}|\{i,j\}\cap(\mathbb{Z}+\frac{1}{2})|}\,U^{|j-i|} - \mathbb{1}_{\{i=j\in\mathbb{Z}\}}. \tag{3}$$

The sphere

We may now prove Propositions 1 and 2. We start with the particular case of the sphere, which is somehow degenerate and has to be treated separately. It is relatively easy and has probably already been done by this method but, as we did not find it in the literature, we do it here for future reference.

The series we consider are really series in $x := t^3$. Setting $\sigma := tF$ and using (1), we obtain that

$$tF = \sigma\,, \qquad \frac{N}{t} = \frac{1}{1-2\sigma}\,, \qquad x = \frac{1}{2}\sigma(1-\sigma)(1-2\sigma). \tag{4}$$

Proof of Propositions 1 and 2 when $\mathcal{S}$ is the sphere. The generating function of rooted encoding mobiles is given by $N/t - 1$ and the generating function of edge-rooted encoding mobiles is given by F^2/t. By Corollary 10 and (1), the generating function of **pointed** plane triangulations is thus

$$\frac{F^2}{t} + 2\left(\frac{N}{t} - 1\right) = \frac{F}{t^2} - 2 = \frac{\sigma}{x} - 2$$

The function σ is an algebraic series in x, which has a dominant singularity at $(12\sqrt{3})^{-1}$ and admits the following Puiseux expansion at its singularity:

$$\sigma = \frac{1}{2} - \frac{\sqrt{3}}{6} - \frac{\sqrt{2}}{6}\big(1 - 12\sqrt{3}\,x\big)^{1/2} + \mathcal{O}\big(1 - 12\sqrt{3}\,x\big). \tag{5}$$

As a result, the generating function of pointed plane triangulations admits the following Puiseux expansion at its singularity:

$$\frac{\sigma}{x} - 2 = 6\sqrt{3} - 8 - 2\sqrt{6}\big(1 - 12\sqrt{3}\,x\big)^{1/2} + \mathcal{O}\big(1 - 12\sqrt{3}\,x\big).$$

By classical transfer theorems [FS09, Chapter VI.3], this implies that the number of plane triangulations with $3n$ edges (and thus $2n$ faces and $n+2$ vertices) is asymptotically equivalent to

$$-\frac{1}{n}\,2\sqrt{6}\,\frac{n^{-3/2}}{\Gamma(-1/2)}\big(12\sqrt{3}\big)^n = \frac{\sqrt{6}}{\sqrt{\pi}}\,n^{-5/2}\big(12\sqrt{3}\big)^n$$

(the factor $1/n$ comes from depointing). This is the statement of Proposition 1.

Proposition 2 is obtained by noticing that the generating function counting plane triangulations with weight x per vertex is given by

$$\int x\left(\frac{\sigma}{x}-2\right)dx = \frac{1}{2}\sigma^3(1-\sigma)(1-4\sigma+2\sigma^2),$$

as claimed. □

The projective plane

We now turn to the projective plane, which is also a degenerate case.

Proof of Propositions 1 and 2 when $\mathcal{S}$ is the projective plane. A unicellular map on the projective plane consists of a single cycle (whose neighborhood forms a Möbius strip) on the vertices of which trees are grafted. We consider an encoding mobile $(\mathfrak{u},\mathfrak{l})$ and we look at the first edge e belonging to the cycle that we meet when traveling along the face of $\mathfrak{u}$ starting from the root. We denote by e_- the extremity of e that we met before visiting e and e_+ the other extremity.

If e is nonflagged, then e_- is necessarily white and e_+ is green. Moreover, e_- is incident to e, another edge of the cycle and two trees, one on each side of the cycle. We cut the cycle at e_-, leaving one of the two trees grafted on each extremity of the chain we obtain. The resulting object is similar to the objects counted by $C_{0,0}$ with the difference that the first N-mobile of the chain is rooted or edge-rooted. Noticing that there are as many nonflagged edges as white corners in any generalized unicellular mobile, we see that counting twice rooted mobiles and once edge-rooted mobiles amounts to counting nonrooted mobiles with a weight twice their number of edges. By Corollary 10, the generating function of pointed triangulations whose corresponding mobile is as considered in this paragraph is thus

$$2t\frac{dN}{dt}\frac{C_{0,0}}{N}.$$

If e is flagged, two cases may happen. If e is not the root edge, then the mobile consists of a chain counted by $C_{\frac{1}{2},\frac{1}{2}}$ together with a rooted or edge-rooted F-mobile. If e is the root edge, then the mobile is obtain by gluing together (in a nonorientable way) the extremities of a nontrivial chain counted by $C_{\frac{1}{2},\frac{1}{2}}$. The generating function of pointed triangulations whose corresponding mobile is as considered in this paragraph is thus

$$C_{\frac{1}{2},\frac{1}{2}}\,2t\frac{dF}{dt} + \frac{C_{\frac{1}{2},\frac{1}{2}}}{t} - 1.$$

A small computation using (2), (3) and (4) yields that the generating function of pointed triangulations on the projective plane is

$$\frac{3}{1-6\sigma+6\sigma^2}\left(\frac{1-2\sigma}{\sqrt{1-6\sigma+6\sigma^2}} - 1 + 2\sigma - 2\sigma^2\right), \tag{6}$$

which has a dominant singularity at $(12\sqrt{3})^{-1}$ and admits the following Puiseux expansion:

$$2^{-3/4}\,3^{5/4}\big(1-12\sqrt{3}\,x\big)^{-3/4}\left(1+\mathcal{O}\big(\big(1-12\sqrt{3}\,x\big)^{1/2}\big)\right).$$

By transfer theorems, the number of triangulations of the projective plane with $3n$ edges (and thus $2n$ faces and $n+1$ vertices) is asymptotically equivalent to

$$\frac{1}{n}\,2^{-3/4}\,3^{5/4}\,\frac{n^{-1/4}}{\Gamma(3/4)}\big(12\sqrt{3}\big)^{n},$$

as desired. The generating function of triangulations counted with weight x per vertex is then given by integrating (6) with respect to x. □

The general case

We suppose from now on that $h \geq 1$, that is, we exclude the already treated cases of the sphere and the projective plane. The general case is similar to [CMS09] (see also [CD15]) so that we only give the main arguments and refer the reader to these references for more detail.

Definition 3. *A* scheme *is a unicellular map of $\mathcal{S}$ with only vertices of degree* 3 *or more. A* normalized scheme *is a pair $(\mathfrak{s},\mathfrak{l}^\star)$ where $\mathfrak{s}$ is a scheme and $\mathfrak{l}^\star : V(\mathfrak{s}) \to \mathbb{Z}_+/2$ is such that, if we denote by $\mathfrak{l}_1^\star < \ldots < \mathfrak{l}_k^\star$ the values of its range, then $\mathfrak{l}_1^\star \in \{0,\frac{1}{2}\}$ and $\mathfrak{l}_{i+1}^\star - \mathfrak{l}_i^\star \in \{\frac{1}{2},1\}$ for $1 \leq i < k$. We denote by $\mathfrak{S}$ the (finite) set of normalized schemes of $\mathcal{S}$.*

We consider an encoding mobile $(\mathfrak{u},\mathfrak{l})$. We denote by $\tilde{\mathfrak{s}}$ its 3-core, that is, the nonrooted unicellular map obtained by iteratively removing from $\mathfrak{u}$ all its vertices of degree 1 and then replacing the chains of edges linking vertices of degree 3 or more by single edges. Note that the vertices of $\tilde{\mathfrak{s}}$ may be green or white and that it is possible that several edges have both extremities that are white vertices. Note also that green vertices of $\tilde{\mathfrak{s}}$ necessarily have degree 3. We give labels to the vertices of $\tilde{\mathfrak{s}}$ as follows: to a white vertex, we give the (integer) label of the corresponding vertex in $\mathfrak{u}$ and to a green vertex, we give the common (noninteger) label of the three flagged edges incident to the corresponding vertex in $\mathfrak{u}$. Let us denote by $\mathfrak{l}_1 < \ldots < \mathfrak{l}_k$ the different values of these labels. We normalize them by replacing them with labels $\mathfrak{l}_1^\star < \ldots < \mathfrak{l}_k^\star$ uniquely defined by $\mathfrak{l}_1^\star \in \{0,\frac{1}{2}\}$, $\mathfrak{l}_{i+1}^\star - \mathfrak{l}_i^\star \in \{\frac{1}{2},1\}$ for $1 \leq i < k$ and $\mathfrak{l}_i^\star - \mathfrak{l}_i \in \mathbb{Z}$ for $1 \leq i \leq k$. We let $\mathfrak{s}$ be the same map as $\tilde{\mathfrak{s}}$ but without distinguishing between green and white vertices and rooted as follows. We start from the root of $\mathfrak{u}$ and we travel along its unique face until we meet a vertex that corresponds to a vertex of $\mathfrak{s}$. The root of $\mathfrak{s}$ is the corner that is visited at this instant, oriented according to the local orientation we were following. The pair $(\mathfrak{s},\mathfrak{l}^\star)$ is then a normalized scheme, which we call *the normalized scheme* of $(\mathfrak{u},\mathfrak{l})$.

At this point, we fix $(\mathfrak{s},\mathfrak{l}^\star) \in \mathfrak{S}$ and we denote by $\mathfrak{l}_1^\star < \ldots < \mathfrak{l}_k^\star$ the values of the range of $\mathfrak{l}^\star$ as above. We will express in terms of U the generating function $P_{(\mathfrak{s},\mathfrak{l}^\star)}$ of pointed triangulations whose encoding mobile has normalized scheme $(\mathfrak{s},\mathfrak{l}^\star)$. We start by arbitrarily associating with every half-edge of $\mathfrak{s}$ an incident corner, and we do this in a bijective way. Let $(\mathfrak{u},\mathfrak{l})$ be a mobile encoding a considered triangulation. Observe that every corner of $\mathfrak{s}$ corresponds to a (possibly empty) tree of $\mathfrak{u}$. We decompose $\mathfrak{u}$ at the vertices corresponding to the vertices of $\mathfrak{s}$ without detaching the previous trees from the associated half-edge. We thus decompose $(\mathfrak{u},\mathfrak{l})$ into a collection of objects that are counted by some $C_{i,j}$'s, one such object per edge of $\mathfrak{s}$. Up to the location of the root, this gives an unequivocal decomposition of $(\mathfrak{u},\mathfrak{l})$. As before, we need to count twice rooted

mobiles and once edge-rooted mobiles, which amounts to counting nonrooted mobiles with a weight twice their number of edges. We let E be the edge set of $\mathfrak{s}$ and, for every edge $e \in E$, we denote by $\mathrm{ind}^-(e)$, $\mathrm{ind}^+(e) \in \{1, \dots, k\}$ the indices such that $\mathfrak{l}^\star_{\mathrm{ind}^-(e)} \le \mathfrak{l}^\star_{\mathrm{ind}^+(e)}$ are the labels of the extremities of e. We thus obtain

$$P_{(\mathfrak{s},\mathfrak{l}^\star)} = \frac{1}{2\,|E|}\, 2t\frac{d}{dt}\left(\sum_{\mathfrak{l}} \prod_{e\in E} C_{\mathfrak{l}_{\mathrm{ind}^-(e)},\mathfrak{l}_{\mathrm{ind}^+(e)}}\right),$$

where the sum is over all labelings whose normalization is $\mathfrak{l}^\star$. The operator $2t\frac{d}{dt}$ counts twice the number of edges and the prefactor comes from the fact that there are $2|E|$ possible re-rootings of $\mathfrak{s}$.

We define the following sets:

$$\begin{aligned}
E^\circ_= &= \big\{e \in E \,:\, \mathfrak{l}^\star_{\mathrm{ind}^-(e)} = \mathfrak{l}^\star_{\mathrm{ind}^+(e)} \in \mathbb{Z}\big\},\\
E^\bullet_= &= \Big\{e \in E \,:\, \mathfrak{l}^\star_{\mathrm{ind}^-(e)} = \mathfrak{l}^\star_{\mathrm{ind}^+(e)} \in \mathbb{Z} + \frac{1}{2}\Big\},\\
E_{\neq} &= \big\{e \in E \,:\, \mathfrak{l}^\star_{\mathrm{ind}^-(e)} \neq \mathfrak{l}^\star_{\mathrm{ind}^+(e)}\big\},\\
V^\bullet &= \Big\{v \in V(\mathfrak{s}) \,:\, \mathfrak{l}^\star(v) \in \mathbb{Z} + \frac{1}{2}\Big\}.
\end{aligned}$$

Using (3) and observing that $\sum_{e\in E} |\{\mathfrak{l}^\star_{\mathrm{ind}^-(e)}, \mathfrak{l}^\star_{\mathrm{ind}^+(e)}\} \cap (\mathbb{Z} + \frac{1}{2})| = 3|V^\bullet|$ (because every vertex in $V^\bullet$ has degree 3), we may express the previous sum as follows.

$$\sum_{\mathfrak{l}} \prod_{e\in E} C_{\mathfrak{l}_{\mathrm{ind}^-(e)},\mathfrak{l}_{\mathrm{ind}^+(e)}} = (B-1)^{|E^\circ_=|}\, B^{|E^\bullet_=|}\, B^{|E_{\neq}|}\, N^{\frac{3}{2}|V^\bullet|} \sum_{\mathfrak{l}} \prod_{e\in E_{\neq}} U^{\mathfrak{l}_{\mathrm{ind}^+(e)} - \mathfrak{l}_{\mathrm{ind}^-(e)}}.$$

Now, the sum in the right-hand side above is equal to

$$\begin{aligned}
\sum_{\mathfrak{l}} \prod_{e\in E_{\neq}} \prod_{j=\mathrm{ind}^-(e)}^{\mathrm{ind}^+(e)-1} U^{\mathfrak{l}_{j+1}-\mathfrak{l}_j} &= \sum_{\delta_1,\dots,\delta_{k-1}\ge 0} \prod_{e\in E_{\neq}} \prod_{j=\mathrm{ind}^-(e)}^{\mathrm{ind}^+(e)-1} U^{\mathfrak{l}^\star_{j+1}-\mathfrak{l}^\star_j+\delta_j}\\
&= \sum_{\delta_1,\dots,\delta_{k-1}\ge 0} \prod_{j=1}^{k-1} U^{d(j)(\mathfrak{l}^\star_{j+1}-\mathfrak{l}^\star_j+\delta_j)}\\
&= \prod_{j=1}^{k-1} \frac{U^{d(j)(\mathfrak{l}^\star_{j+1}-\mathfrak{l}^\star_j)}}{1-U^{d(j)}}
\end{aligned}$$

where we set $d(j) := |\{e \in E_{\neq} \,:\, \mathrm{ind}^-(e) \le j < \mathrm{ind}^+(e)\}|$ for $1 \le j < k$. Summing up and expressing everything in terms of U with the help of (2), we obtain

$$P_{(\mathfrak{s},\mathfrak{l}^\star)} = \frac{2^{|E^\circ_=|}}{|E|}\, 3x\frac{d}{dx}\left(\frac{U^{|E^\circ_=|+\frac{1}{2}|V^\bullet|}\,(1+U)^{|E|-|E^\circ_=|-|V^\bullet|}}{(1-U)^{|E|}} \prod_{j=1}^{k-1} \frac{U^{d(j)(\mathfrak{l}^\star_{j+1}-\mathfrak{l}^\star_j)}}{1-U^{d(j)}}\right). \tag{7}$$

By the Euler characteristic formula, a triangulation of $\mathcal{S}$ with $3n$ edges has $n+2-2h$ vertices. The generating functions of pointed triangulations and of triangulations of $\mathcal{S}$ are thus respectively

$$\sum_{(\mathfrak{s},\mathfrak{l}^\star)\in\mathfrak{S}} P_{(\mathfrak{s},\mathfrak{l}^\star)} \qquad \text{and} \qquad \sum_{(\mathfrak{s},\mathfrak{l}^\star)\in\mathfrak{S}} \int x^{1-2h} P_{(\mathfrak{s},\mathfrak{l}^\star)}\, dx\,. \tag{8}$$

The leading contributions in the asymptotic formula will come from normalized schemes $(\mathfrak{s}, \mathfrak{l}^\star)$ that maximize both the number of edges of $\mathfrak{s}$ and the cardinality of the range of $\mathfrak{l}^\star$. It is not very hard to see that such normalized schemes are the ones where the scheme is cubic, that is, with only vertices of degree 3, and the labeling function is injective. Moreover, such schemes all have $6h-3$ edges and $4h-2$ vertices. See [CD15, Lemma 4.3] for a proof of these facts. We denote by $\mathfrak{S}^\star \subseteq \mathfrak{S}$ the set of these normalized schemes.

Proposition 11. *We suppose here that $h \geq 1$. The constant $c_{\mathcal{S}}$ of Proposition 1 is given by*

$$c_{\mathcal{S}} = \frac{2^{-(13h-9)/2}\, 3^{-5(h-1)/2}}{(6h-3)\,\Gamma\big((5h-3)/2\big)} \left(\sum_{(\mathfrak{s},\mathfrak{l}^\star)\in\mathfrak{S}^\star} 2^{-|V^\bullet|} \prod_{j=1}^{4h-3} \frac{1}{d(j)} \right).$$

Proof of Proposition 1 when $h \geq 1$ and of Proposition 11. Let $(\mathfrak{s}, \mathfrak{l}^\star) \in \mathfrak{S}$ and let k denote the cardinality of the range of $\mathfrak{l}^\star$ as above. The generating function $P_{(\mathfrak{s},\mathfrak{l}^\star)}$ admits a unique dominant singularity at $x = (12\sqrt{3})^{-1}$, which corresponds to a singularity of U and at the same time to a value where $U = 1$. Moreover, at this singularity, $1-U$ admits the following Puiseux expansion:

$$1 - U = 2^{5/4}\, 3^{1/4} \big(1 - 12\sqrt{3}\, x\big)^{1/4} + \mathcal{O}\big(\big(1 - 12\sqrt{3}\, x\big)^{1/2}\big)\,.$$

As a result,

$$[x^n] P_{(\mathfrak{s},\mathfrak{l}^\star)} \sim \frac{2^{-(|E|+4|V^\bullet|+5k-5)/4}\, 3^{-(|E|+k-5)/4}}{|E|\,\Gamma\big((|E|+k-1)/4\big)} \left(\prod_{j=1}^{k-1} \frac{1}{d(j)} \right) n^{(|E|+k-1)/4} \big(12\sqrt{3}\big)^n\,.$$

The leading contributions are thus obtained for normalized schemes maximizing $|E|+k$ as we claimed. The number of triangulations of $\mathcal{S}$ with $3n$ edges is thus asymptotically equivalent to

$$\frac{1}{n} \sum_{(\mathfrak{s},\mathfrak{l}^\star)\in\mathfrak{S}} [x^n] P_{(\mathfrak{s},\mathfrak{l}^\star)} \sim \frac{2^{-(13h-9)/2}\, 3^{-5(h-1)/2}}{(6h-3)\,\Gamma\big((5h-3)/2\big)} \left(\sum_{(\mathfrak{s},\mathfrak{l}^\star)\in\mathfrak{S}^\star} 2^{-|V^\bullet|} \prod_{j=1}^{4h-3} \frac{1}{d(j)} \right) n^{5(h-1)/2} \big(12\sqrt{3}\big)^n$$

as desired. □

For $h = 1$, the expression of $c_{\mathcal{S}}$ becomes

$$c_{\mathcal{S}} = \frac{1}{12} \left(\sum_{(\mathfrak{s},\mathfrak{l}^\star)\in\mathfrak{S}^\star} \frac{1}{2^{|V^\bullet|}\, d(1)} \right).$$

If $\mathcal{S}$ is the torus, there is only one possible scheme, consisting of 3 edges linking 2 vertices. In this case, $d(1) = 3$ for every scheme and the possible labelings, starting from the root vertex, are $(0,1)$, $(0,\frac{1}{2})$, $(\frac{1}{2},1)$, $(\frac{1}{2},\frac{3}{2})$ and the symmetrical pairs. As a result,

$$c_{\mathcal{S}} = \frac{1}{12}\frac{2}{3}\left(1 + \frac{1}{2} + \frac{1}{2} + \frac{1}{4}\right) = \frac{1}{8}.$$

If $\mathcal{S}$ is the Klein bottle, there are two types of possible schemes obtained as follows. We consider a hexagon with sides denoted by s_1, s_2, …, s_6 in clockwise order around it. We glue together s_1

with s_4 in an orientable way. The first type of schemes is then obtained by gluing in a nonorientable way s_2 with s_6 and s_3 with s_5. The second type of schemes is obtained by gluing in a nonorientable way s_2 with s_3 and s_5 with s_6. For the first type of scheme, $d(1) = 3$ and for the second type of scheme, there are two loops so that $d(1) = 1$. In both cases, the labels can be $\{0, 1\}$, $\{0, \frac{1}{2}\}$, $\{\frac{1}{2}, 1\}$ or $\{\frac{1}{2}, \frac{3}{2}\}$ with 6 possible rootings. All in all,

$$c_{\mathcal{S}} = \frac{1}{12}\, 6 \left(1 + \frac{1}{3}\right)\left(1 + \frac{1}{2} + \frac{1}{2} + \frac{1}{4}\right) = \frac{3}{2}.$$

This completes the values given in Table 1.

Proof of Proposition 2 when $h = 1$. By (7) and (8), the generating function of triangulations when $h = 1$ is

$$\sum_{(\mathfrak{s},\mathfrak{l}^\star)\in\mathfrak{S}} 3\, \frac{2^{|E^\circ_=|}\, U^{|E^\circ_=| + \frac{1}{2}|V^\bullet|}\, (1+U)^{|E| - |E^\circ_=| - |V^\bullet|}}{|E|\, (1-U)^{|E|}} \prod_{j=1}^{k-1} \frac{U^{d(j)(\mathfrak{l}^\star_{j+1} - \mathfrak{l}^\star_j)}}{1 - U^{d(j)}}.$$

Let us start with the torus. There are 11 normalized schemes on the torus. There is one with one vertex labeled 0 and 2 edges: its contribution in the sum is $6U^2(1-U)^{-2}$. The 10 remaining ones all have the same scheme with 2 vertices linked by 3 edges. The different labelings and the corresponding contributions are presented in Table 2.

$\left(\frac{1}{2}, \frac{1}{2}\right)$	$\left(\frac{1}{2}, \frac{3}{2}\right)$, $\left(\frac{3}{2}, \frac{1}{2}\right)$	$\left(0, \frac{1}{2}\right)$, $\left(\frac{1}{2}, 0\right)$, $\left(1, \frac{1}{2}\right)$, $\left(\frac{1}{2}, 1\right)$	$(0,0)$	$(0,1)$, $(1,0)$
$\frac{U(1+U)}{(1-U)^3}$	$\frac{U^4(1+U)}{(1-U^3)(1-U)^3}$	$\frac{U^2(1+U)^2}{(1-U^3)(1-U)^3}$	$\frac{8U^3}{(1-U)^3}$	$\frac{U^3(1+U)^3}{(1-U^3)(1-U)^3}$

Table 2: *The contributions of all the normalized schemes of the torus except the one with only one vertex. The labeling is given as a pair whose first coordinate is the label of the root vertex and the second coordinate is the label of the other vertex.*

Summing these contributions, we obtain that the generating function of triangulations on the torus is equal to

$$\frac{U(U^2 + 10U + 1)}{(1-U)^4} = \frac{\sigma(1-\sigma)}{2\left(1 - 6\sigma + 6\sigma^2\right)^2}.$$

On the Klein bottle, the normalized schemes are as follows. There is one with one vertex labeled 0 and 2 twisted edges and 2 with one vertex labeled 0, one twisted edge and one straight edge. These 3 normalized schemes all have contribution $6U^2(1-U)^{-2}$. The remaining normalized schemes all have a scheme of one the two types presented before this proof. Moreover, for any given nonrooted such normalized scheme with a root vertex prescribed, there are 3 possible rootings. The contributions of the normalized schemes of the first type are the same as for the torus, that is, the ones of Table 2. For the normalized schemes of the second type, the contributions are presented in Table 3.

$\left(\frac{1}{2},\frac{1}{2}\right)$	$\left(\frac{1}{2},\frac{3}{2}\right)$, $\left(\frac{3}{2},\frac{1}{2}\right)$	$\left(0,\frac{1}{2}\right)$, $\left(\frac{1}{2},0\right)$, $\left(1,\frac{1}{2}\right)$, $\left(\frac{1}{2},1\right)$	$(0,0)$	$(0,1)$, $(1,0)$
$\frac{U(1+U)}{(1-U)^3}$	$\frac{U^2(1+U)}{(1-U)^4}$	$\frac{2U^2(1+U)}{(1-U)^4}$	$\frac{8U^3}{(1-U)^3}$	$\frac{4U^3(1+U)}{(1-U)^4}$

Table 3: *The contributions of the normalized schemes of the second type on the Klein bottle. The labeling is given as a pair whose first coordinate is the label of the root vertex and the second coordinate is the label of the other vertex.*

The generating function of triangulations on the Klein bottle is thus equal to

$$\frac{6U(13U^2+10U+1)}{(1-U)^4} = \frac{3\sigma(1-\sigma)\big(7-30\sigma+30\sigma^2-6(1-2\sigma)\sqrt{1-6\sigma+6\sigma^2}\big)}{\big(1-6\sigma+6\sigma^2\big)^2}.$$

□

A Representation of unicellular maps as polygons with paired sides

It is sometimes convenient to represent a unicellular map $\mathfrak{u}$ as a polygon with twice as many sides as the number of edges of $\mathfrak{u}$. In this representation, the sides of the polygon are paired either in an orientable way or in a nonorientable way (see Figure 20).

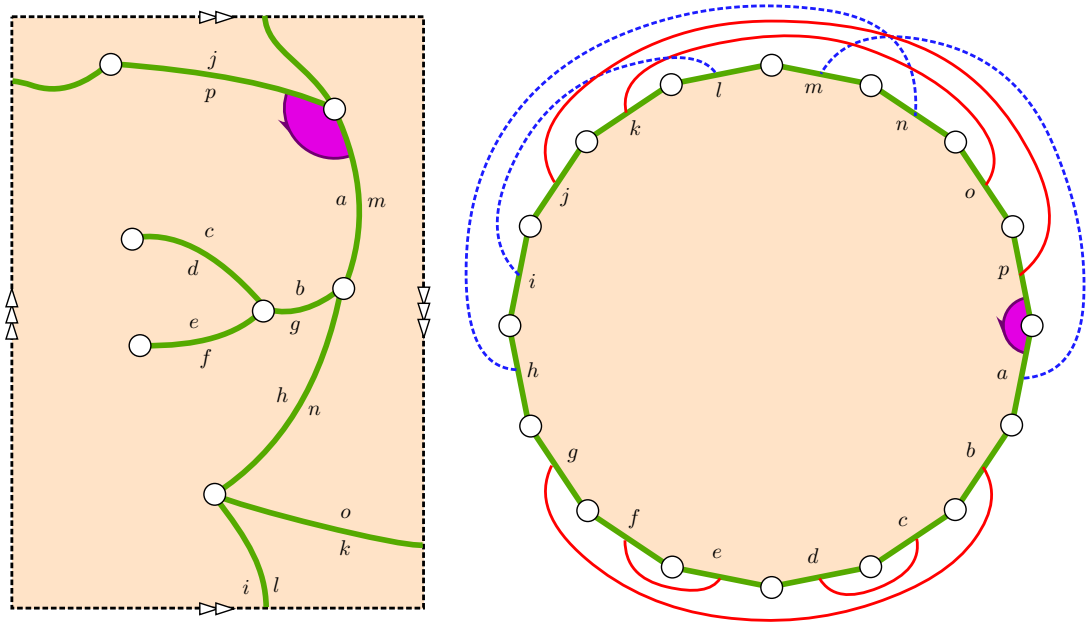

Figure 20: *Representation of a unicellular map as a polygon with paired sides. The red straight lines correspond to orientable pairings and the dashed blue lines correspond to nonorientable pairings. The letters are positioned according to the contour order of the unique face.*

In this appendix, we use this representation for Figures 7, 9, 12 and 14.

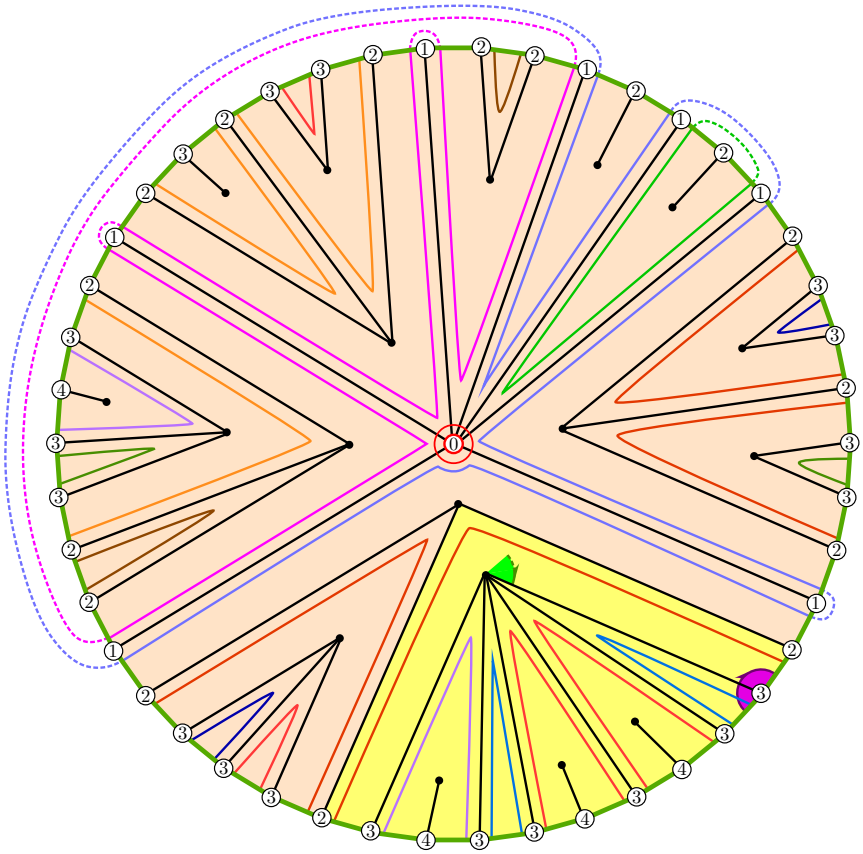

Figure 21: *Polygon representation of Figure 7. We represented the identifications of the loops at level* 1 *on the paired sides by dashed lines (regardless of the orientability of the pairings). For a better visibility, the side pairings are not represented; the unicellular map is the one from Figure 6.*

References

[AB13] Jan Ambjørn and Timothy G. Budd. Trees and spatial topology change in causal dynamical triangulations. *J. Phys. A*, 46(31):315201, 33, 2013.

[ABA13] Louigi Addario-Berry and Marie Albenque. The scaling limit of random simple triangulations and random simple quadrangulations. *Preprint*, arXiv: 1306. 5227, 2013.

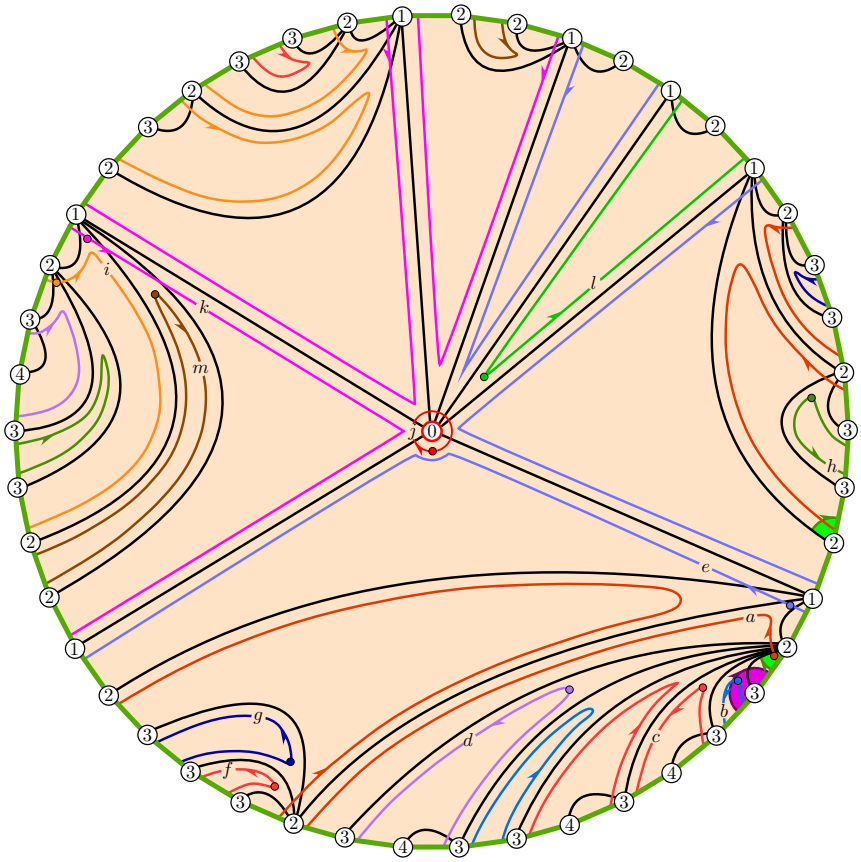

Figure 22: *Polygon representation of Figure 9. The Chapuy–Dołęga bijection, from a well-labeled unicellular map to a pointed bipartite quadrangulation.*

[Abr13] Céline Abraham. Rescaled bipartite planar maps converge to the Brownian map. *Preprint*, arXiv: 1312. 5959, 2013.

[BC86] Edward A. Bender and E. Rodney Canfield. The asymptotic number of rooted maps on a surface. *J. Combin. Theory Ser. A*, 43(2):244–257, 1986.

[BCD16] Jérémie Bettinelli, Guillaume Chapuy, and Maciej Dołęga. Nonorientable Brownian surfaces. *In preparation*, 2016.

[BDG02] Jérémie Bouttier, Philippe Di Francesco, and Emmanuel Guitter. Census of planar maps: from the one-matrix model solution to a combinatorial proof. *Nuclear Phys. B*, 645(3):477–499, 2002.

[BDG04] Jérémie Bouttier, Philippe Di Francesco, and Emmanuel Guitter. Planar maps as labeled mobiles. *Electron. J. Combin.*, 11(1):Research Paper 69, 27 pp. (electronic), 2004.

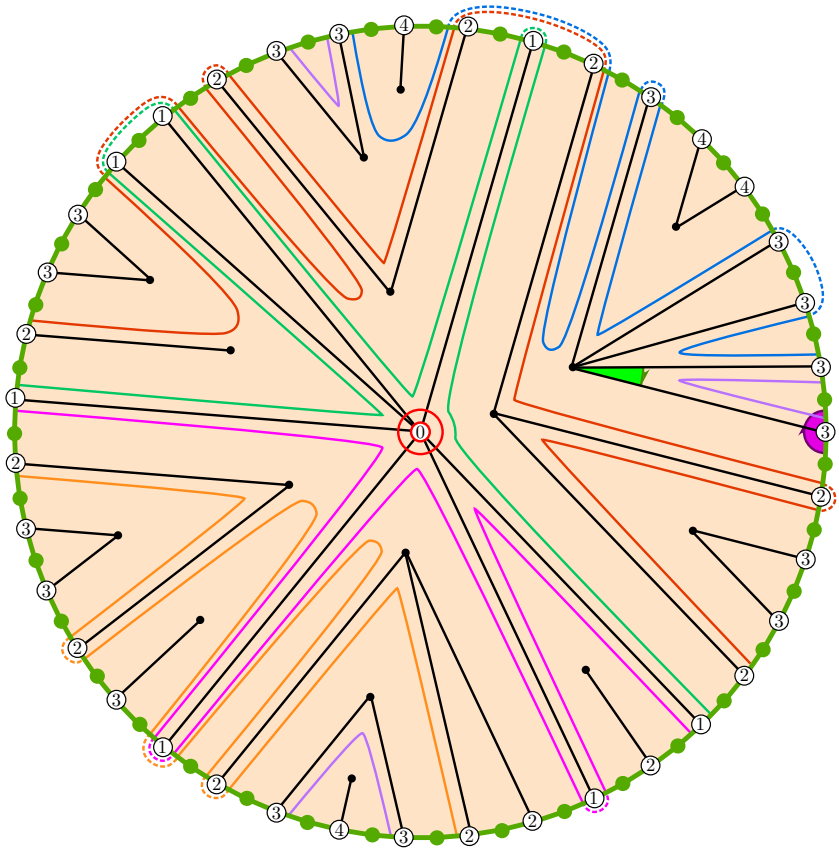

Figure 23: *Polygon representation of Figure 12. A few identifications along side pairings are represented by dashed lines.*

[Bet14] Jérémie Bettinelli. Geodesics in Brownian surfaces (Brownian maps). *Preprint*, arXiv: 1401. 3602, *to appear in Ann. Inst. Henri Poincaré Probab. Stat.*, 2014.

[BJM14] Jérémie Bettinelli, Emmanuel Jacob, and Grégory Miermont. The scaling limit of uniform random plane maps, *via* the Ambjørn–Budd bijection. *Electron. J. Probab.*, 19:no. 74, 1–16, 2014.

[BLG13] Johel Beltran and Jean-François Le Gall. Quadrangulations with no pendant vertices. *Bernoulli*, 19(4):1150–1175, 2013.

[BM15] Jérémie Bettinelli and Grégory Miermont. Compact Brownian surfaces I. Brownian disks. *Preprint*, arXiv: 1507. 08776, 2015.

[BM16] Jérémie Bettinelli and Grégory Miermont. Compact Brownian surfaces II. The general case. *In preparation*, 2016.

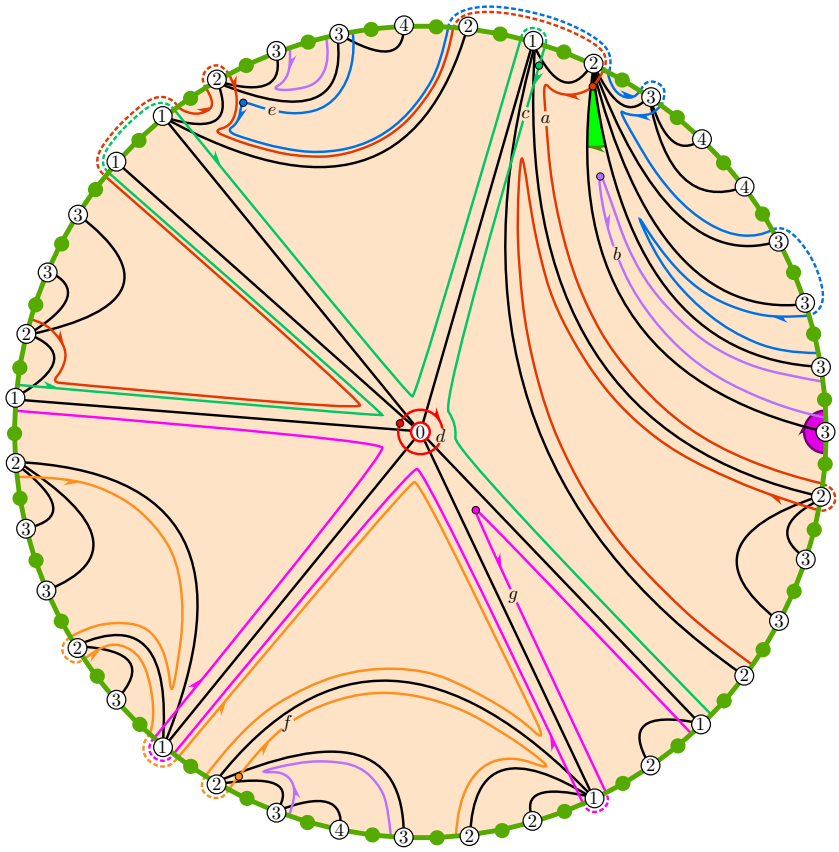

Figure 24: *Polygon representation of Figure 14. The bijection, from a well-labeled unicellular mobile to a pointed bipartite map.*

[CD15] Guillaume Chapuy and Maciej Dołęga. A bijection for rooted maps on general surfaces. *Preprint*, arXiv: 1501. 06942, 2015.

[Cha09] Guillaume Chapuy. Asymptotic enumeration of constellations and related families of maps on orientable surfaces. *Combin. Probab. Comput.*, 18(4):477–516, 2009.

[CMS09] Guillaume Chapuy, Michel Marcus, and Gilles Schaeffer. A bijection for rooted maps on orientable surfaces. *SIAM J. Discrete Math.*, 23(3):1587–1611, 2009.

[CV81] Robert Cori and Bernard Vauquelin. Planar maps are well labeled trees. *Canad. J. Math.*, 33(5):1023–1042, 1981.

[Eyn12] Bertrand Eynard. *Counting surfaces*. Birkhauser, 2012.

[FS09] Philippe Flajolet and Robert Sedgewick. *Analytic combinatorics*. Cambridge University Press, Cambridge, 2009.

[Gao91] Zhicheng Gao. The number of rooted triangular maps on a surface. *J. Combin. Theory Ser. B*, 52(2):236–249, 1991.

[Gao93] Zhicheng Gao. The number of degree restricted maps on general surfaces. *Discrete Math.*, 123(1-3):47–63, 1993.

[LG13] Jean-François Le Gall. Uniqueness and universality of the Brownian map. *Ann. Probab.*, 41(4):2880–2960, 2013.

[Mie13] Grégory Miermont. The Brownian map is the scaling limit of uniform random plane quadrangulations. *Acta Math.*, 210(2):319–401, 2013.

[PS06] Dominique Poulalhon and Gilles Schaeffer. Optimal coding and sampling of triangulations. *Algorithmica*, 46(3-4):505–527, 2006.

[Sch98] Gilles Schaeffer. *Conjugaison d'arbres et cartes combinatoires aléatoires*. PhD thesis, Université de Bordeaux 1, 1998.

[Tut63] William T. Tutte. A census of planar maps. *Canad. J. Math.*, 15:249–271, 1963.